C.2

LOS ALAMOS SCIENTIFIC LABORATORY
OF THE UNIVERSITY OF CALIFORNIA ○ LOS ALAMOS NEW MEXICO

METHODS OF DIFFERENCING IN EULERIAN HYDRODYNAMICS

LEGAL NOTICE

LOS ALAMOS SCIENTIFIC LABORATORY
OF THE UNIVERSITY OF CALIFORNIA   LOS ALAMOS   NEW MEXICO

REPORT WRITTEN: February 1959

REPORT DISTRIBUTED: April 11, 1960

METHODS OF DIFFERENCING IN EULERIAN HYDRODYNAMICS

By

H. Jerry Longley

CONTENTS

ILLUSTRATIONS

INTRODUCTION

Methods of differencing the Eulerian form of the hydrodynamic equations are investigated. One wishes to find a method for machine calculations that could be used in hydrodynamic problems involving large distortions of matter in two space dimensions. Boundaries between materials are to be carried and moved through the fixed Eulerian mesh. Given a mesh at some time and with proper boundary conditions, the problem will be to carry the values of the quantities stored in each mesh point forward in time explicitly to a small time δt later. The problem will first be discussed in one space dimension and then for the case of two dimensions. This numerical method is for compressible flow in the presence of shocks. The IBM Electronic Data Processing Machine, Type 704, was used for the numerical computations.

The hydrodynamic equations for mass flow, momentum change, and energy change are, respectively:

$$\frac{\partial \rho}{\partial t} = - \nabla \cdot \rho \vec{V} \tag{1}$$

$$\rho \frac{d\vec{V}}{dt} = - \nabla p \tag{2}$$

$$\rho \, \frac{dE}{dt} = - \, \nabla \cdot (p\vec{V}) \qquad\qquad (3)$$

where ρ is the density, $\vec{V}$ is the material velocity, p is the pressure, and E is the total energy per unit mass. E is the sum of the internal energy per unit mass $(\mathcal{E})$ and the kinetic energy per unit mass, i.e., $E = \mathcal{E} + \frac{1}{2} \vec{V} \cdot \vec{V}$.

CHAPTER I

DIFFERENCING IN ONE DIMENSION

Values of ρ_j, V_j, and $\mathcal{E}_j$ will be considered as the value of ρ, V, and $\mathcal{E}$, respectively, at the center of the jth cell of the mesh. Strictly speaking, the product of ρ_j and the volume of the jth cell is the mass in the jth cell. The product of V_j and the product of E_j with this mass are the momentum and energy, respectively, in the jth cell. For a one-dimensional space mesh, a simple method of differencing Eq. (1) $\left(\frac{\partial \rho}{\partial t} = - \frac{\partial (\rho V)}{\partial x} \right)$ in the jth cell would yield

$$\rho_j^{n+1} - \rho_j^n = + \frac{\delta t}{\delta x} \left\{ (\rho V)_{j-1/2}^n - (\rho V)_{j+1/2}^n \right\} \tag{4}$$

where $(\rho V)_{j+1/2}^n$ is the value selected for (ρV) on the right boundary of the jth cell and $(\rho V)_{j-1/2}^n$ is the value on the left. By n is meant that the quantity is to be evaluated from the mesh values at time step n, and n+1 is the value resulting from the solution of Eq. (4) at a time δt later (one time step later).

-1 | 1 | 2 | ... | j-1 | j | j+1 | ... | JM-1 | JM | JM+1

$\leftarrow \delta x \rightarrow$

$J \rightarrow$

$j-\frac{1}{2}$ $j+\frac{1}{2}$
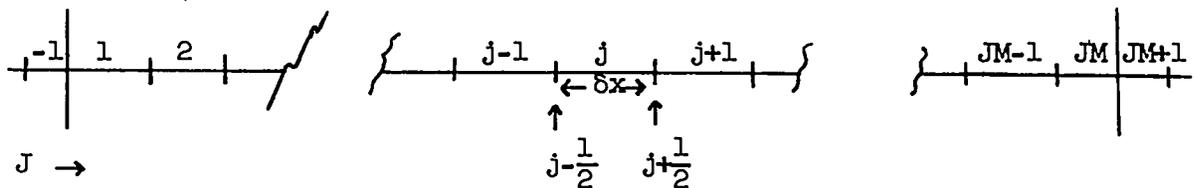
Figure 1

Equation (4) is in the form which we will call <u>conservative</u>. The value of the flow quantity, (ρV), on the right boundary of cell j is the same value used on the left side for cell j+1. To illustrate a result obtainable from Eq. (4), we take a box (Figure 1) with no flow out either end, i.e., $(\rho V)_{1-1/2} = (\rho V)_{JM+1/2} = 0$. Then we find from Eq. (4) that

$$\sum_{j=1}^{JM} \delta x_j \left(\rho_j^{n+1} - \rho_j^n \right) = 0$$

analytically, i.e., mass is conserved exactly. It has been explicitly assumed that $(\rho V)_{j+1/2}$ in cell j is equal $(\rho V)_{j-1/2}$ for cell j+1, i.e., the flow term (ρV) is single valued on a cell boundary. If $(\rho V)_{1-1/2}$ and/or $(\rho V)_{JM+1/2}$ are not zero, then the mass of the system will be changing as specified by the boundary conditions on these boundary values. It may be noted that Eq. (4) is conservative regardless of how $(\rho V)_{j-1/2}$ and $(\rho V)_{j+1/2}$ are evaluated when $(\rho V)_{j+1/2}$ for cell j is equal $(\rho V)_{j-1/2}$ for cell j+1.

Assuming one starts at j = 1, with suitable boundary values for $(\rho V)_{1-1/2}$ and $(\rho V)_{JM+1/2}$, the problem of evaluating ρ_j^{n+1} in Eq. (4) becomes one of evaluating $(\rho V)_{j+1/2}$ in each cell j. $(\rho V)_{j-1/2}$ will have already been calculated in the preceding cell by the same method used in

calculating $(\rho V)_{j+1/2}$ in the present cell and will be used in a conservative manner. Starting at $j = JM$, the situation is simply reversed.

Equations (2) and (3) are not in the form for conservative differencing. Remembering that for a scalar φ, $\frac{d\varphi}{dt} = \frac{\partial\varphi}{\partial t} + \bar{V} \cdot \nabla\varphi$, Eq. (2) in one dimension becomes

$$\rho \frac{\partial V}{\partial t} + \rho V \frac{\partial V}{\partial x} = - \frac{\partial p}{\partial x}$$

Adding $V \frac{\partial \rho}{\partial t}$ to both sides and using Eq. (1),

$$\frac{\partial(\rho V)}{\partial t} = - \frac{\partial p}{\partial x} - (\rho V) \frac{\partial V}{\partial x} - V \frac{\partial(\rho V)}{\partial x} = - \frac{\partial(p + \rho V^2)}{\partial x}$$

Equation (3) is changed to conservative form similar to Eq. (2) and in differential form gives

$$\frac{\partial(\rho E)}{\partial t} = - \frac{\partial(p V + \rho V E)}{\partial x}$$

Thus, in conservative difference form, Eqs. (1), (2), and (3) are written

$$\rho_j^{n+1} - \rho_j^n = \frac{\delta t}{\delta x} \left\{ (\rho V)_{j-1/2}^n - (\rho V)_{j+1/2}^n \right\} \tag{4}$$

$$\rho_j^{n+1} V_j^{n+1} - \rho_j^n V_j^n = \frac{\delta t}{\delta x} \left\{ (p + \rho V^2)_{j-1/2}^n - (p + \rho V^2)_{j+1/2}^n \right\} \tag{5}$$

and

$$\rho_j^{n+1} E_j^{n+1} - \rho_j^n E_j^n = \frac{\delta t}{\delta x} \left\{ (pV + \rho VE)_{j-1/2}^n - (pV + \rho VE)_{j+1/2}^n \right\} \quad (6)$$

This system of equations will be solved after finding a difference method for the flow quantities on the right side of a cell in the order presented. That is, ρ_j^{n+1} from Eq. (4) will be used to solve for V_j^{n+1} in Eq. (5); ρ_j^{n+1} and V_j^{n+1} will then be used to solve for ε_j^{n+1} $\left[E_j^{n+1} = \varepsilon_j^{n+1} + \frac{1}{2} (V_j^{n+1})^2 \right]$ in Eq. (6). The solution of Eqs. (4), (5), and (6) for all mesh points is called the n + 1 calculation.

Two difficulties in solving the above system of difference equations are related to their stability and their behavior in attempting to represent shock discontinuities. The method of von Neumann and Richtmyer[1] to solve both of these difficulties is to introduce a fictitious bulk-viscosity pressure, Q, and to replace the material pressure in the above equations by the material pressure plus Q. This viscosity spreads the shock region and thus turns the discontinuity into a region of continuity and gives stability to the other regions of flow because of its second order effects.

We will consider viscosity pressures of the form $Q = - \sigma \frac{\partial V}{\partial x}$. Four types of particular interest will be characterized by

$$\sigma_{RV} = C_1 \frac{\delta x^2}{2} \rho \left| \frac{\partial V}{\partial x} \right| \quad (7)$$

$$\sigma_{LA} = C_1 \frac{\delta x}{2} \rho C \tag{8}$$

$$\sigma_{pic} = C_1 \frac{\delta x}{2} \rho |V| \tag{9}$$

and

$$\sigma_{LO} = C_{LO} p \tag{10}$$

σ_{RV} gives the Richtmyer-von Neumann[1] type viscosity. σ_{LA} gives the Landshoff[2] type viscosity when C is the sound speed. σ_{pic} gives the effective viscosity of the "particle-in-cell" method.[3] σ_{LO} is a type viscosity introduced in this paper with two-dimensional machine calculations in mind. σ_{LO} depends on the temperature, as does C, but does not require taking a square root as does C. C_1 is a constant used to set the magnitude of the viscosity term. C_{LO} is also a constant. C_{LO} is determined by equating σ_{LA} (with C_1 given) and σ_{LO} in some region and at some time for the problem at hand. If the values of p, ρ, and C in the desired region and at the desired time are given by $\bar{p}$, $\bar{\rho}$, and $\bar{C}$, respectively, then $C_{LO} = C_1 \frac{\delta x \bar{\rho} \bar{C}}{2 \bar{p}}$. In the piston problem to be presented, the values of $\bar{p}$, $\bar{\rho}$, and $\bar{C}$ were the theoretically expected values taken from the reflected shock region.

A stability criterion[1] for the present system which is not unconditionally unstable is not the most pertinent consideration for selecting δt. Experience has shown that δt will have to be roughly ten times smaller than required by the stability requirement to give good accuracy.

Let M ($= \frac{|V|}{C}$) be the Mach number. For $M \geq 1$, δt will have to be selected in such a manner that matter will require roughly ten time steps to cross a cell. For $M \leq 1$, the selection of δt is to be made so that the sound wave takes roughly ten time steps to cross a cell.

Second-order terms may be added to Eqs. (1) and (3) which effectively spread the shock and have the same stabilizing effect that the term Q does in Eq. (2). We will consider in one dimension a mass diffusion term in Eq. (1) and a heat conduction term in Eq. (3). It should be noted that while the replacement of p by the material pressure plus Q results in a dissipative term[3] in Eq. (3), this term does not have the form of heat conduction.

The quantities on the right boundary of a cell in Eqs. (4), (5), and (6) will be designated by

$$(\rho V)_{j+1/2} = (\rho_a V_a) - C_o D_{j+1/2} (\rho_{j+1} - \rho_j) \tag{11}$$

$$(p + \rho VV)_{j+1/2} = p_a + Q + (\rho_b V_b) \cdot V_d \tag{12}$$

$$(pV + \rho VE)_{j+1/2} = (p_b + Q) V_e + (\rho_c V_c) E_a$$

$$- C_2 H_{j+1/2} (\mathcal{E}_{j+1} - \mathcal{E}_j) \tag{13}$$

where each separate appearance of ρ, V, p, and E is distinguished by an alphabetic letter as a subscript. These alphabetically subscripted terms

are ρ_a, V_a, P_a, ρ_b, V_b, V_d, P_b, V_e, ρ_c, V_c, and E_a. Each of these terms, as discussed in the next paragraph, will be evaluated on the $j + 1/2$ boundary of the cell j. $D_{j+1/2}$ is the portion of the explicitly added mass diffusion term which is to be considered a function of ρ, V, and $\mathcal{E}$; $H_{j+1/2}$ is the corresponding function in the heat conduction term. C_o is the constant appearing in the explicitly added mass diffusion term; C_2 is the corresponding constant in the heat conduction term. Q is the explicitly added viscosity term as designated by Eqs. (7), (8), (9), or (10).

We now consider various differencing types. Let f_j represent any single alphabetically subscripted quantity other than the explicitly added diffusion terms represented in Eqs. (11), (12), or (13) in the jth cell. The types of differencing of these terms considered here will be

Type I: $f_{j+1/2} = \dfrac{f_j + f_{j+1}}{2}$

Type II: $f_{j+1/2} \begin{cases} = f_j & \text{if} \quad V_T > 0 \\ \\ = 0 & \text{if} \quad V_T = 0 \\ \\ = f_{j+1} & \text{if} \quad V_T < 0 \end{cases}$

<u>Type III:</u>

$$f_{j+1/2} \begin{cases} = (6f_j + 3f_{j+1} - f_{j-1})/8 & \text{if} \quad V_T > 0 \\ \\ = 0 & \text{if} \quad V_T = 0 \\ \\ = (6f_{j+1} + 3f_j - f_{j+2})/8 & \text{if} \quad V_T < 0 \end{cases}$$

<u>Type IV:</u>

$$f_{j+1/2} \begin{cases} = (4f_j + f_{j+1} - f_{j-1})/4 & \text{if} \quad V_T > 0 \\ \\ = 0 & \text{if} \quad V_T = 0 \\ \\ = (4f_{j+1} + f_j - f_{j+2})/4 & \text{if} \quad V_T < 0 \end{cases}$$

Type I gives a linear differencing scheme. For Types II, III, and IV, we define the <u>selected cell</u> to be j if $V_T > 0$ or to be $j + 1$ if $V_T < 0$. V_T, a test flow value, is usually taken as $V_T = (V_j + V_{j+1})$. Thus, j is the selected cell if the flow is to the right and $j + 1$ if the flow is to the left at $j + 1/2$. Type II indicates that one is to use the value in the selected cell as the value on the boundary. Type III is the result of a quadratic fit of $f(x)$, centered in the selected cell, using the values in the selected cell and the two contiguous cells and evaluated for x on the $j + 1/2$ boundary. Type IV is an extrapolation from the value in the selected cell to the $j + 1/2$ boundary using the slope given by the cells on both sides of the selected cell. It may be

noted that all four types of differencing schemes can be characterized by three numbers, say, ξ_1, ξ_2, and ξ_3. If one writes

$$f_{j+1/2} \begin{cases} = \dfrac{\xi_1 f_j + \xi_2 f_{j+1} + \xi_3 f_{j-1}}{\xi_1 + \xi_2 + \xi_3} & \text{if} \quad V_T > 0 \\[4mm] = 0 & \text{if} \quad V_T = 0 \\[4mm] = \dfrac{\xi_1 f_{j+1} + \xi_2 f_j + \xi_3 f_{j+2}}{\xi_1 + \xi_2 + \xi_3} & \text{if} \quad V_T < 0 \end{cases}$$

then one has the correspondence

Type	ξ_1	ξ_2	ξ_3
I	1	1	0
II	1	0	0
III	6	3	-1
IV	4	1	-1

In the present work, $V_T = (V_j + V_{j+1})$ is used to evaluate V_a from one of the above schemes. The resultant value of V_a is used as the test value when differencing any of the other alphabetically subscripted terms. Obviously, only Type I differencing of p_a will be considered, i.e., one would not set the pressure to zero on a cell boundary if the velocity were zero at that point.

The preceding paragraph merely outlines the prescription for carrying out the various differencing schemes. At this point, it seems appropriate to give a somewhat more detailed discussion of the significance of the last three schemes from both the mathematical and physical points of view.

Type II differencing gives a diffusion or second order effect. For $V_T > 0$ on both sides of a cell, the derivative of f in cell j will be represented as

$$\frac{\partial f}{\partial x_j} = \frac{f_j - f_{j-1}}{\delta x}$$

which would normally be called the derivative of f at $j - 1/2$. An expansion, $f'(x + h) = f'(x) + h \cdot f''(x) + \frac{h^2}{2!} f'''(x) + \ldots$, yields $f'_{j-1/2}$ $= f'_j - \frac{\delta x}{2} f''_j(x)$ when only the first order correction term is used. Correspondingly, for $V_T < 0$ on both sides of the cell, we find $f'_{j+1/2} = f'_j$ $+ \frac{\delta x}{2} f''_j(x)$. Thus, for $V_T = $ a constant, $V_T \frac{\partial f}{\partial x}$ would be given by

$$V_T \frac{\partial f}{\partial x_j} = V_T f'_j - \left| V_T \right| \frac{\delta x}{2} f''_j$$

for Type II differencing. If V_a were a constant in Eq. (11) and ρ_a were treated by Type II differencing, then a mass diffusion term would result from this differencing. If V_a were not constant and also given Type II differencing, a more complicated type of second order velocity term would also be present. Differencing V_d in Eq. (12) and E_a in Eq. (13) by Type II gives second order effects in the pic method.[3]

Type III differencing gives a fitting of the derivatives, i.e., for $V_T > 0$ on both sides,

$$\frac{\partial f}{\partial x_j} = \frac{6(f_j - f_{j-1}) + 3(f_{j+1} - f_j) - (f_{j-1} - f_{j-2})}{8\delta x}$$

$$= (6f'_{j-1/2} + 3f'_{j+1/2} - f'_{j-3/2})/8$$

If $V_T < 0$ on both sides, then $f'_{j+3/2}$ is used in the derivative fit. Type IV is similar except that it uses extrapolation of the derivative. If $V_T > 0$ on the right and $V_T < 0$ on the left of cell j, then Types III and IV give

$$\frac{\partial f}{\partial x_j} = \frac{f_{j+1} - f_{j-1}}{2\delta x}$$

On the other hand, if $V_T < 0$ on the right and $V_T > 0$ on the left of cell j, then Type III gives

$$\frac{\partial f}{\partial x_j} = \frac{3}{2}\left[\frac{f_{j+1} - f_{j-1}}{2\delta x}\right] - \frac{1}{2}\left[\frac{f_{j+2} - f_{j-2}}{4\delta x}\right]$$

and Type IV gives

$$\frac{\partial f}{\partial x_j} = 2\left[\frac{f_{j+1} - f_{j-1}}{2\delta x}\right] - 1\left[\frac{f_{j+2} - f_{j-2}}{4\delta x}\right]$$

When V_T has different signs on opposite sides of a cell, we have a so-called stagnation region (low velocity region). The last three equations show how $\frac{\partial f}{\partial x}$ in the jth cell would be calculated from Types III and IV differencing in a stagnation region. Since these latter calculations use ordinary linear type differencing for the derivatives, or weighted combinations, there are no diffusion effects from Types III and IV differencing in a stagnation region.

The first test problem selected for machine calculation was that of a steady state infinite shock moving to the right and in the leftmost cell at time zero. This is called the piston problem. The right side of the rightmost cell (JM) was selected to be a rigid wall so that the reflected shock could be studied. The application of the Hugoniot relations in this problem and in the fractured diaphragm problem to be presented later, are given elsewhere[4] and will not be discussed in detail in this paper. These theoretical steady state solutions will be given on the graphs as straight lines. A polytropic gas will be assumed. We set $\xi = b\Theta$ and $p = k\rho\Theta$, where b is the specific heat at constant volume, k is the gas constant, and Θ is the temperature. We take b = 0.06 and k = 0.04 so that $\gamma(= 1 + \frac{k}{b})$ is $\frac{5}{3}$. In front of the shock the temperature and velocity are zero and the density is unity. The Hugoniot relations then give $\rho_s = 4$, $\Theta_s = 8\frac{1}{3}$, and the shock velocity (V_s) equals 4/3 when the material velocity behind the shock is unity. Thus, at the left boundary and to the left of this point, the conditions are given by $\rho_{-1} = \rho_{1-1/2} = 4$, $V_{-1} = V_{1-1/2} = 1$, and $\Theta_{-1} = \Theta_{1-1/2} = 8\frac{1}{3}$. The

condition for reflection at the boundary JM + 1/2 is satisfied by setting $V_{JM+1} = -V_{JM}$, $\Theta_{JM+1} = \Theta_{JM}$, and $\rho_{JM+1} = \rho_{JM}$. It may be noted that, regardless of the differencing scheme considered here, these conditions insure no mass flow, $(\rho V)_{JM+1/2} = 0$, and no energy flow, $(pV + \rho VE)_{JM+1/2} = 0$, out of the system at the JM + 1/2 boundary. Also, all diffusion terms vanish except for Q at JM + 1/2.

Figures 2 through 29 show some of the results of various differencing methods for the piston problem. In all these examples, $p_a = p_b$, $\rho_a = \rho_b = \rho_c$, and $V_a = V_b = V_c$. Some test problems were run using $p_a \neq p_b$ and leaving Q out of Eq. (13), but all such problems gave poorer results than the ones shown. Poorer results were also obtained when the mass flow terms were not kept equal. We set $(\rho_a V_a) = (\rho_b V_b) = (\rho_c V_c)$ by the above equality of the individual ρ's and V's. Whole terms, as contrasted to individual factors, were differenced by the above-mentioned types without any significant improvements. An example of this sort would be to take $(\rho_a V_a) = f_{i+1/2}$ and select Types I, II, III, or IV differencing for this whole term.

When the calculation for Q results in a negative number, one generally considers that there is a rarefaction region, i.e., $\frac{\partial V}{\partial x} > 0$. Since one does not wish to spread a rarefaction region, the Q should be cut off (Q = 0) if it is negative. The word cut after the viscosity designation on the graphs means that a test on $\frac{\partial V}{\partial x}$ was performed and Q was set to zero if $\frac{\partial V}{\partial x} > 0$. The explicit heat diffusion term, characterized by

Figure 2

Term	Type	
ρ_a	I	$C_0 = 0$
V_a	I	$C_1 = 6.0, \ \sigma_{RV}$
P_a	I	$C_2 = 0$
V_d	I	
E_a	I	
V_e	I	

$X (\delta X = 1)$
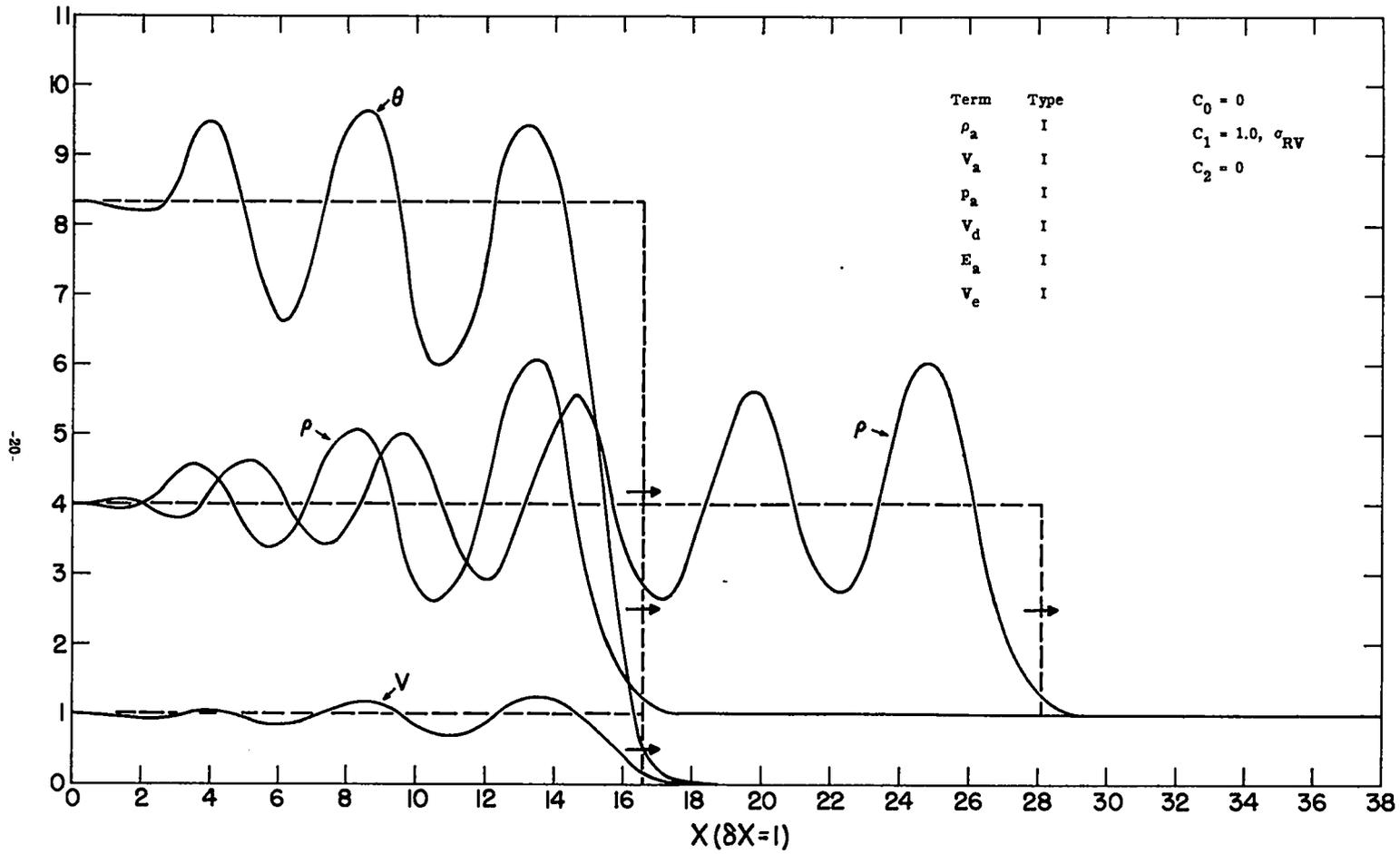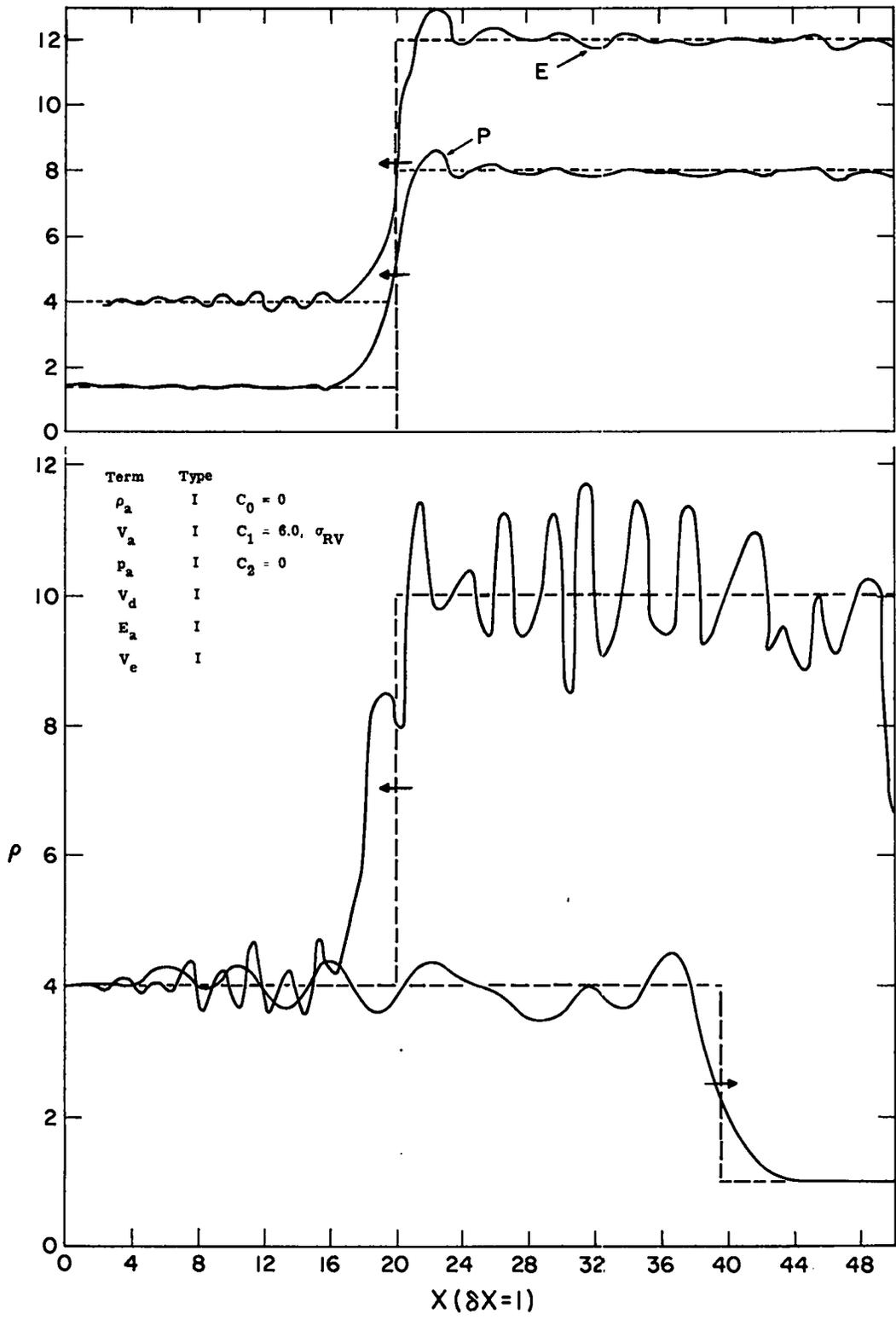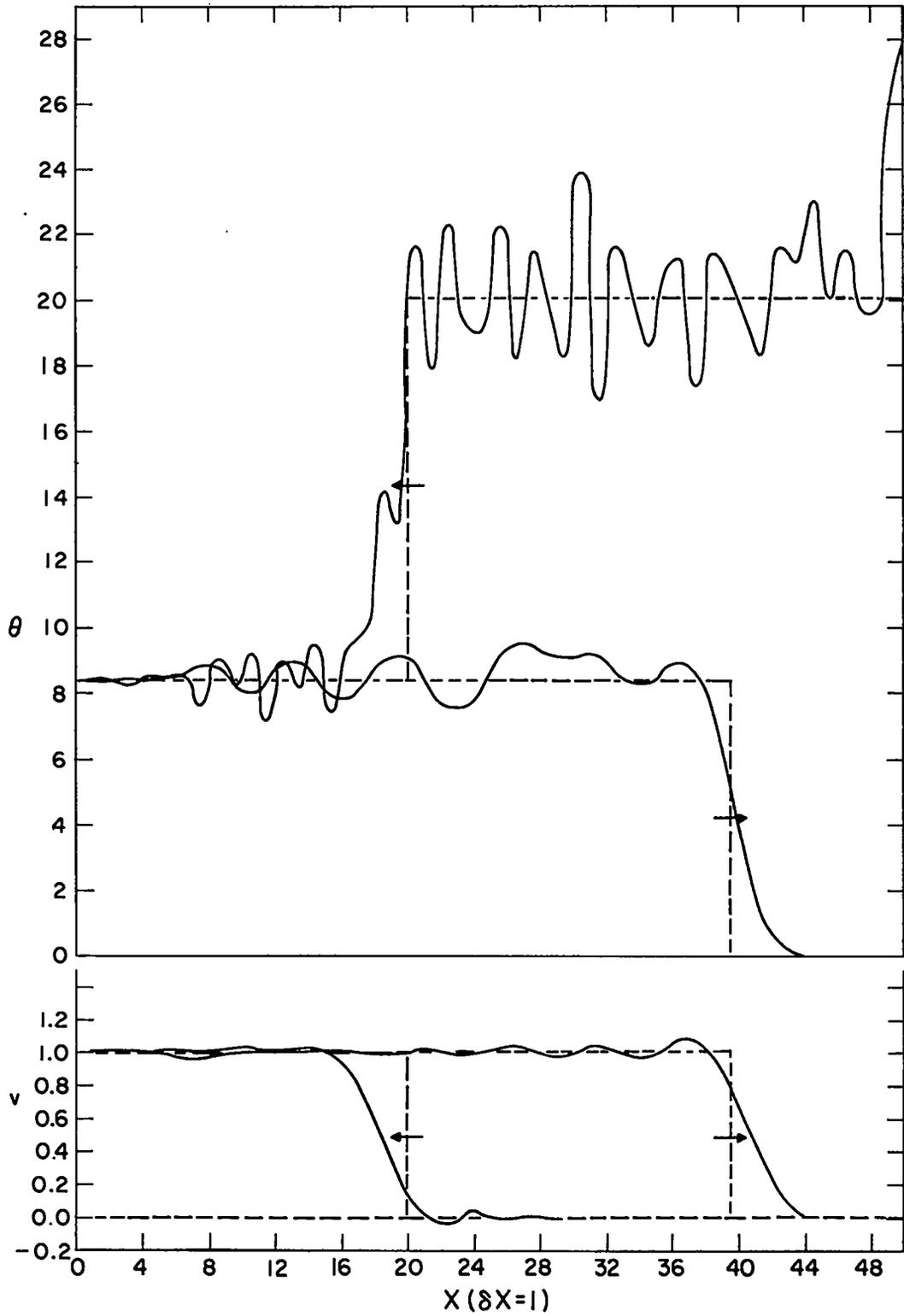
Figure 3A
-21-

Figure 3B
-22-
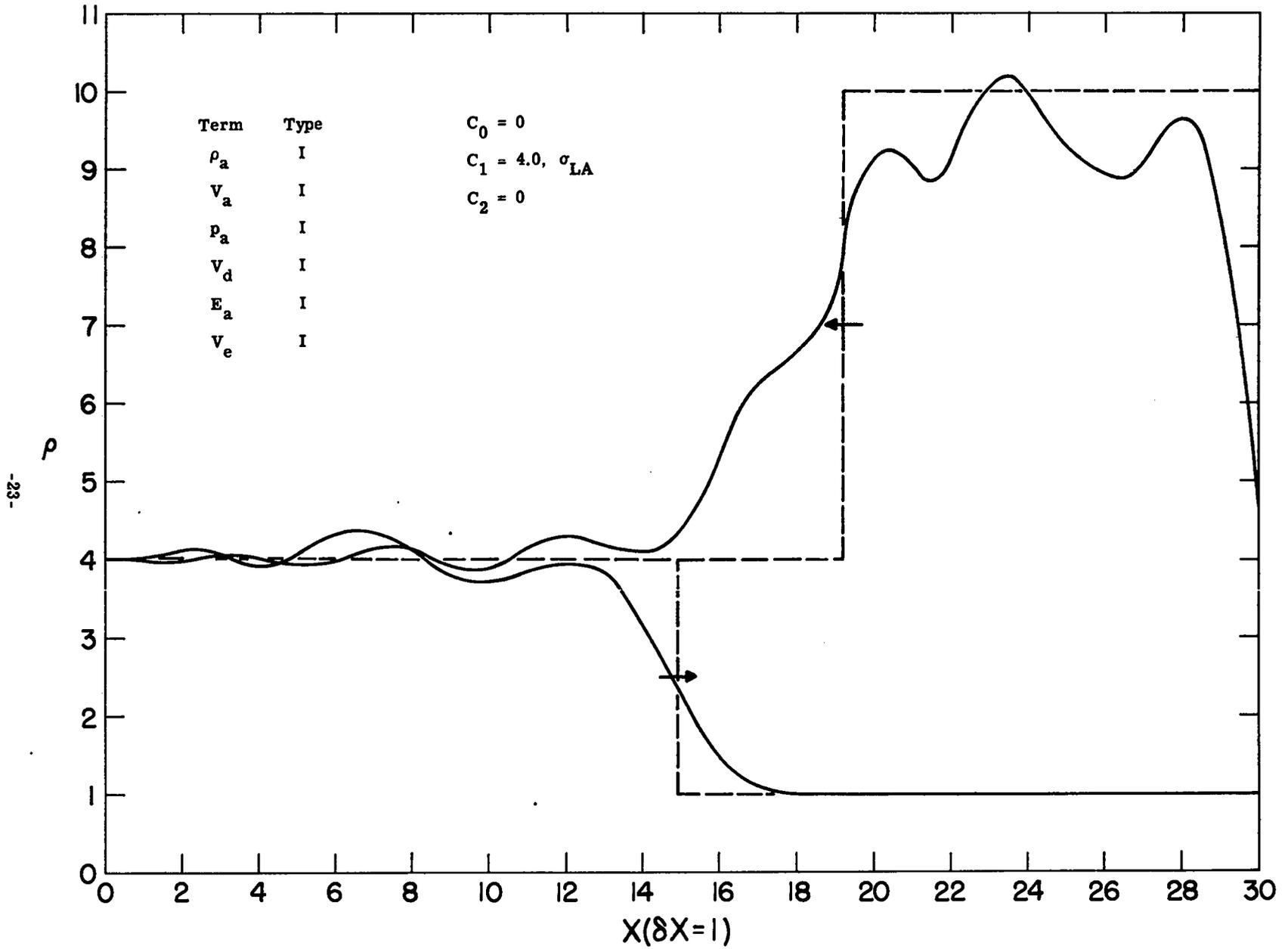
Figure 4

Figure 5

Figure 6
-25-

Term	Type
ρ_a	II
V_a	I
p_a	I
V_d	II
E_a	II
V_e	I

$C_0 = 0$

$C_1 = 0$

$C_2 \neq 0$

ρ

$X\ (\delta X = 1)$

Figure 7

Term	Type
ρ_a	II
V_a	I
p_a	I
V_d	II
E_a	II
V_e	I

$C_0 = 0$

$C_1 = 0.5, \; \sigma_{LO}$

$C_2 = 0$

ρ

$X(\delta X = 1)$
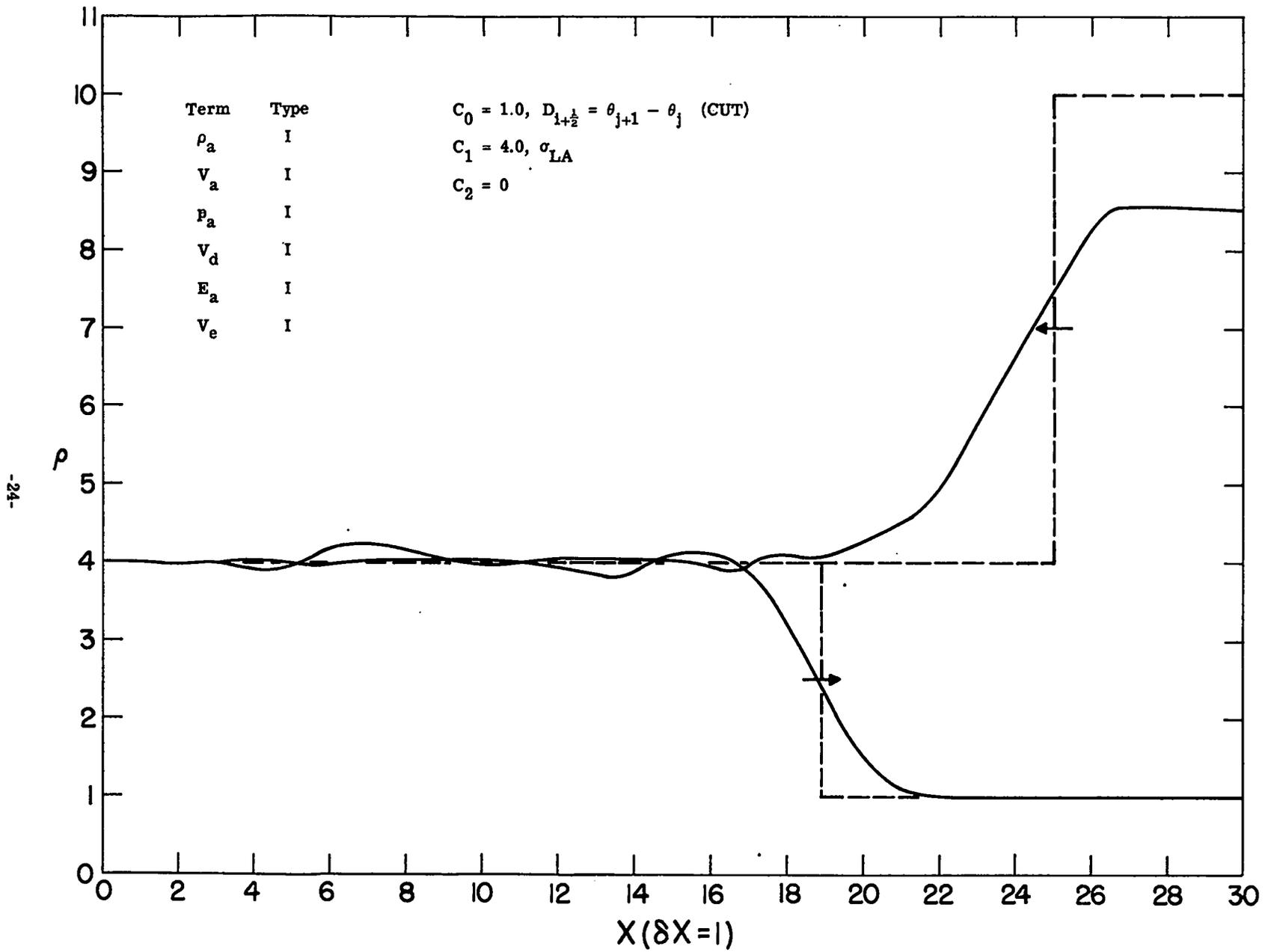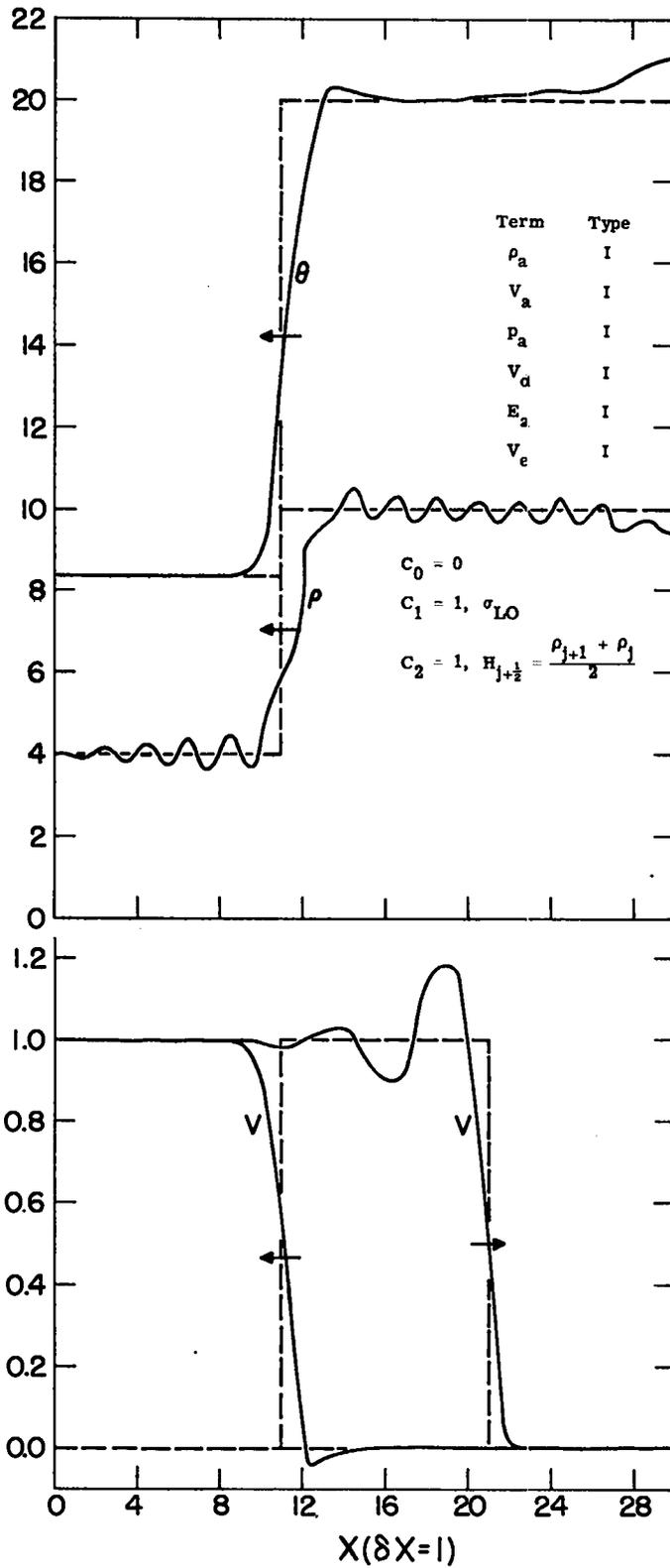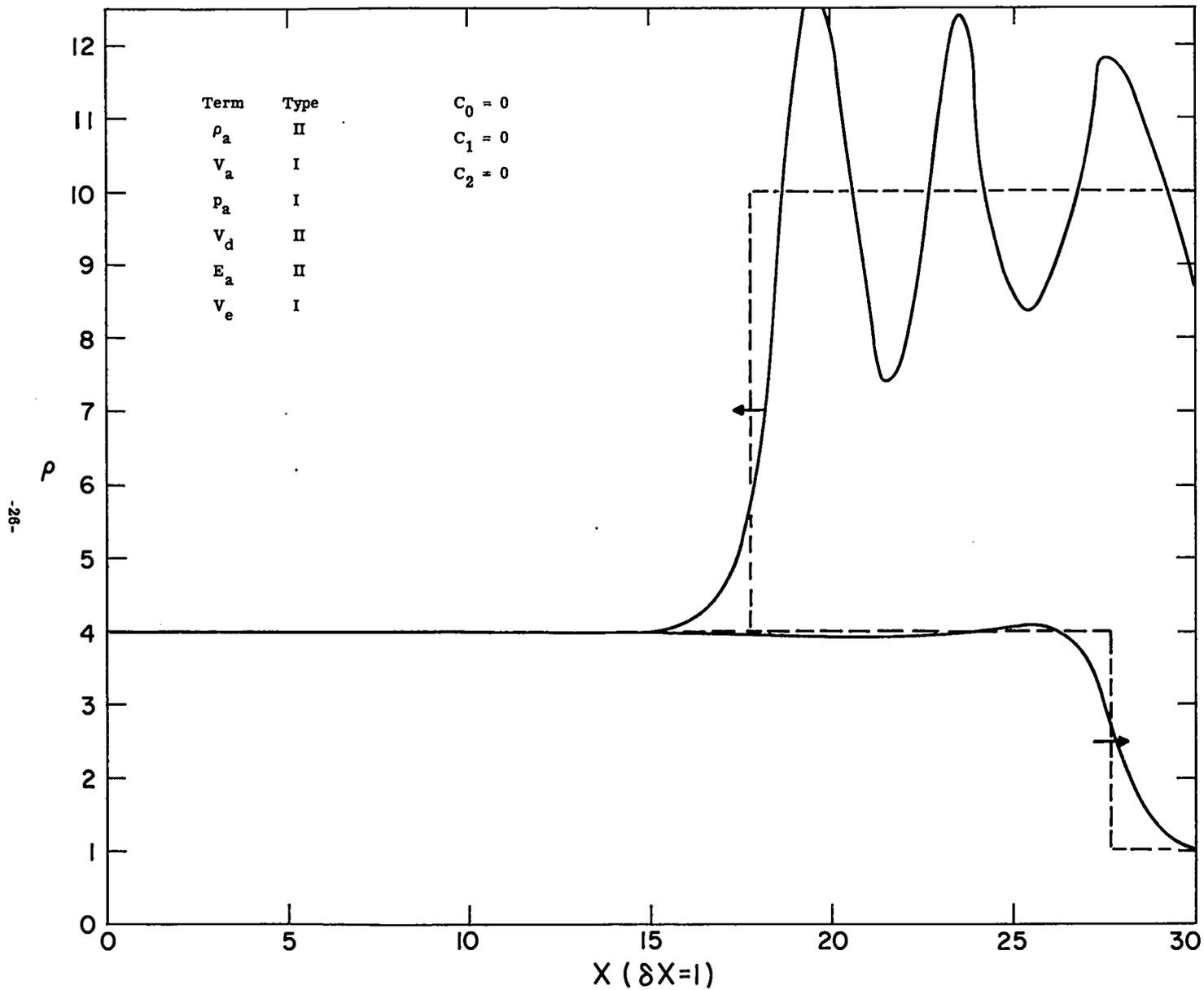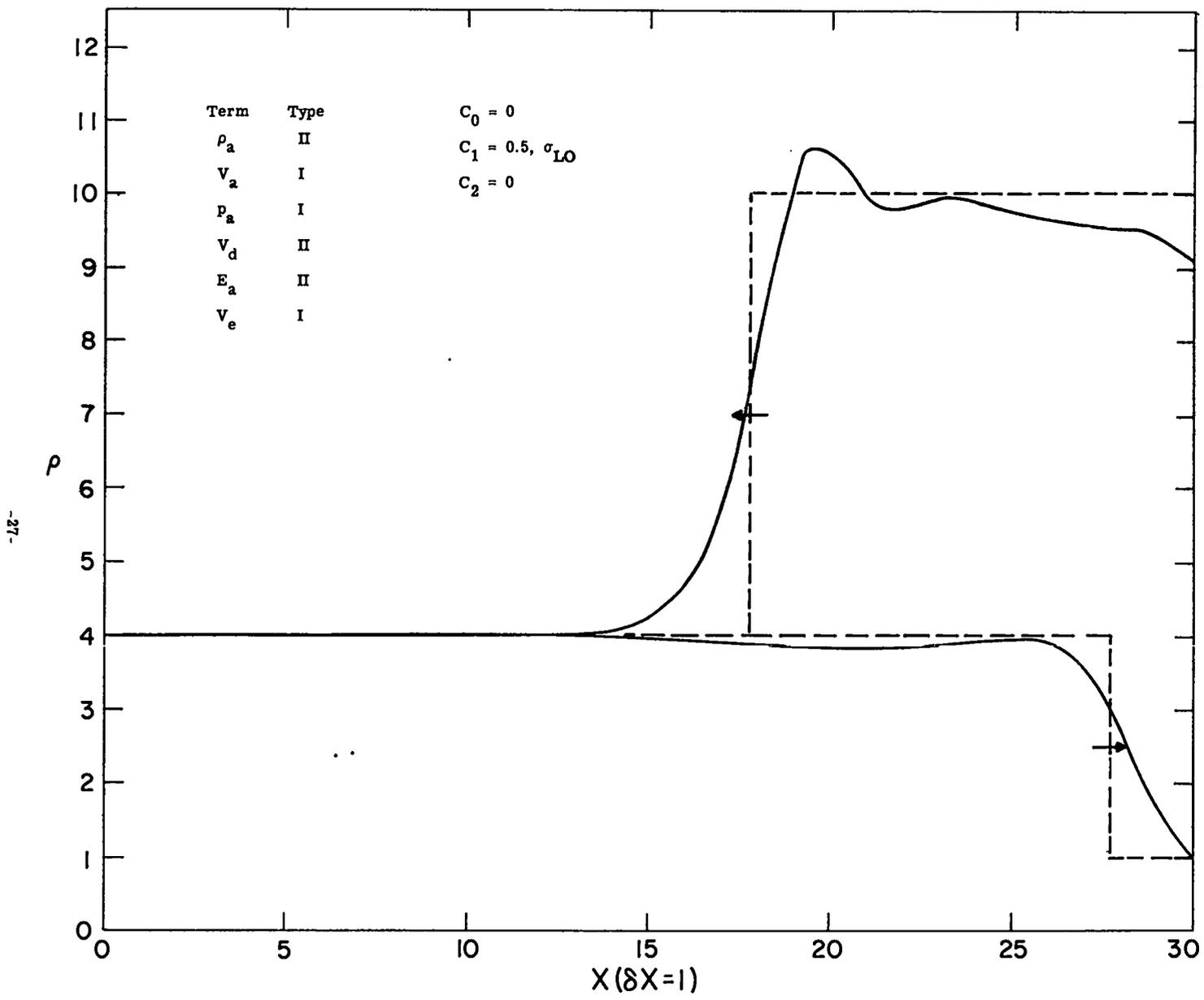
Figure 8

Figure 9

Figure 10

Term	Type
ρ_a	I
V_a	I
p_a	I
V_d	II
E_a	II
V_e	I

$C_0 = 0$

$C_1 = 0$

$C_2 = 0$

DID NOT REFLECT
(UNBOUNDED)

ρ

$X (\delta X = 1)$
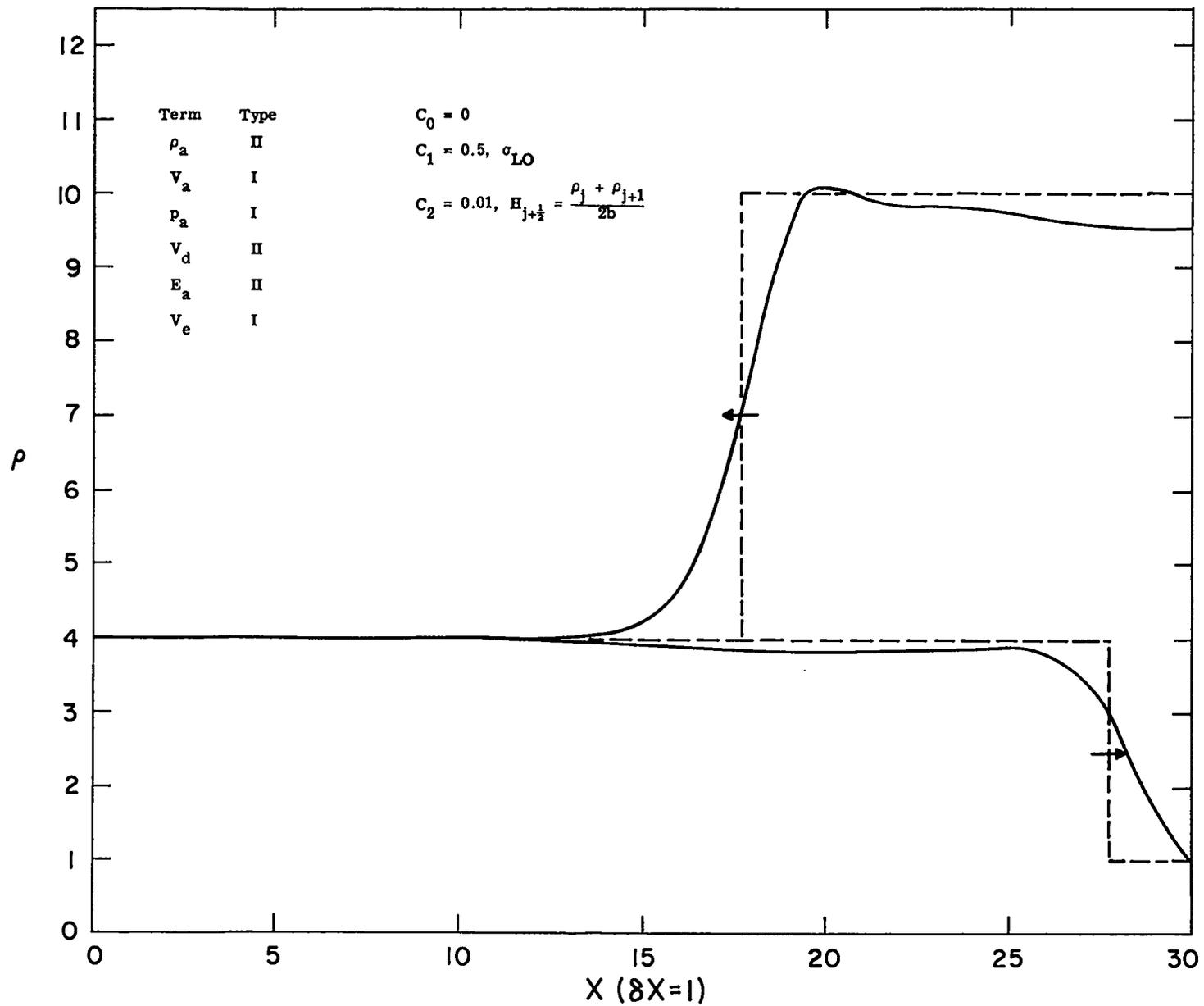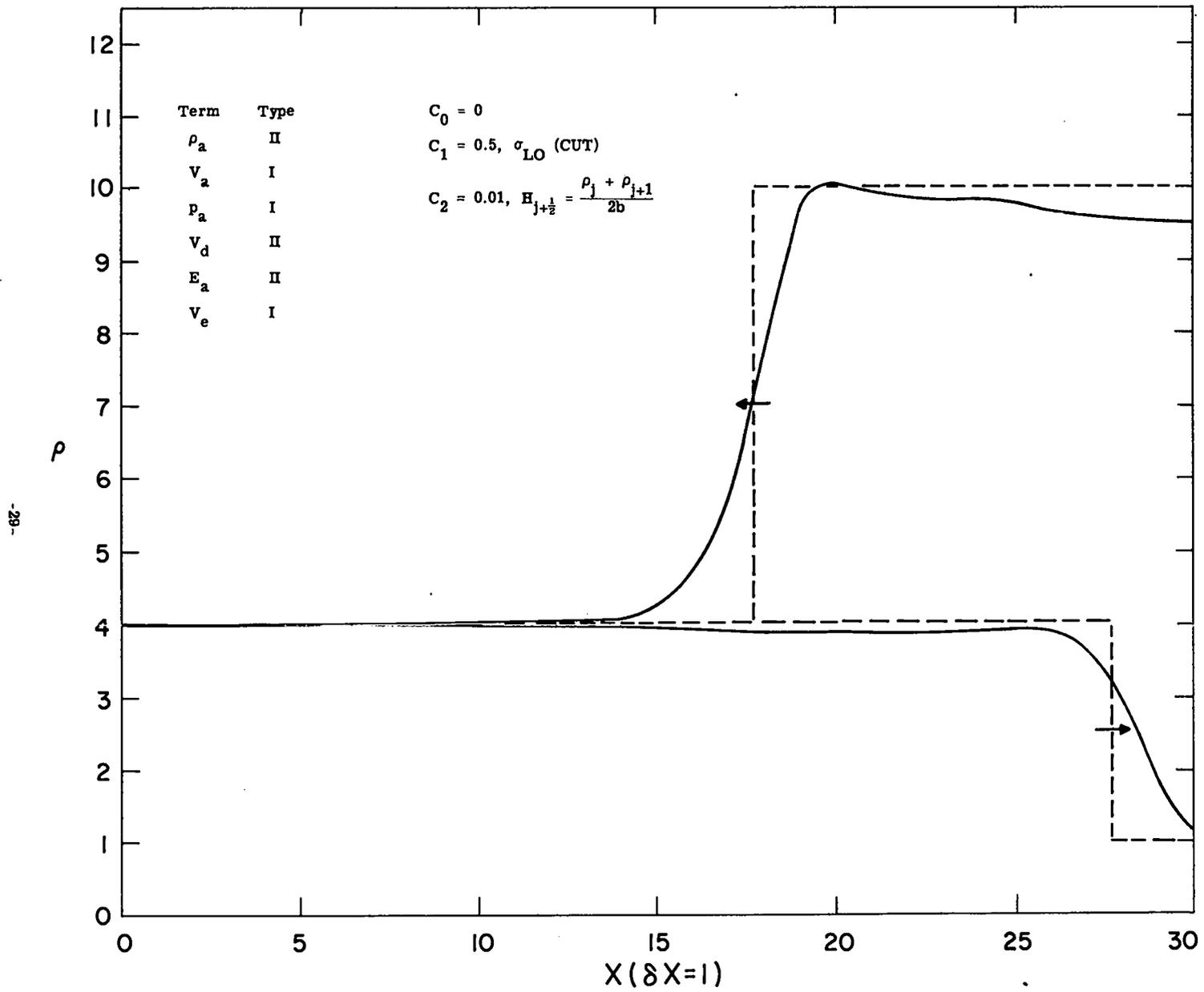
-30-
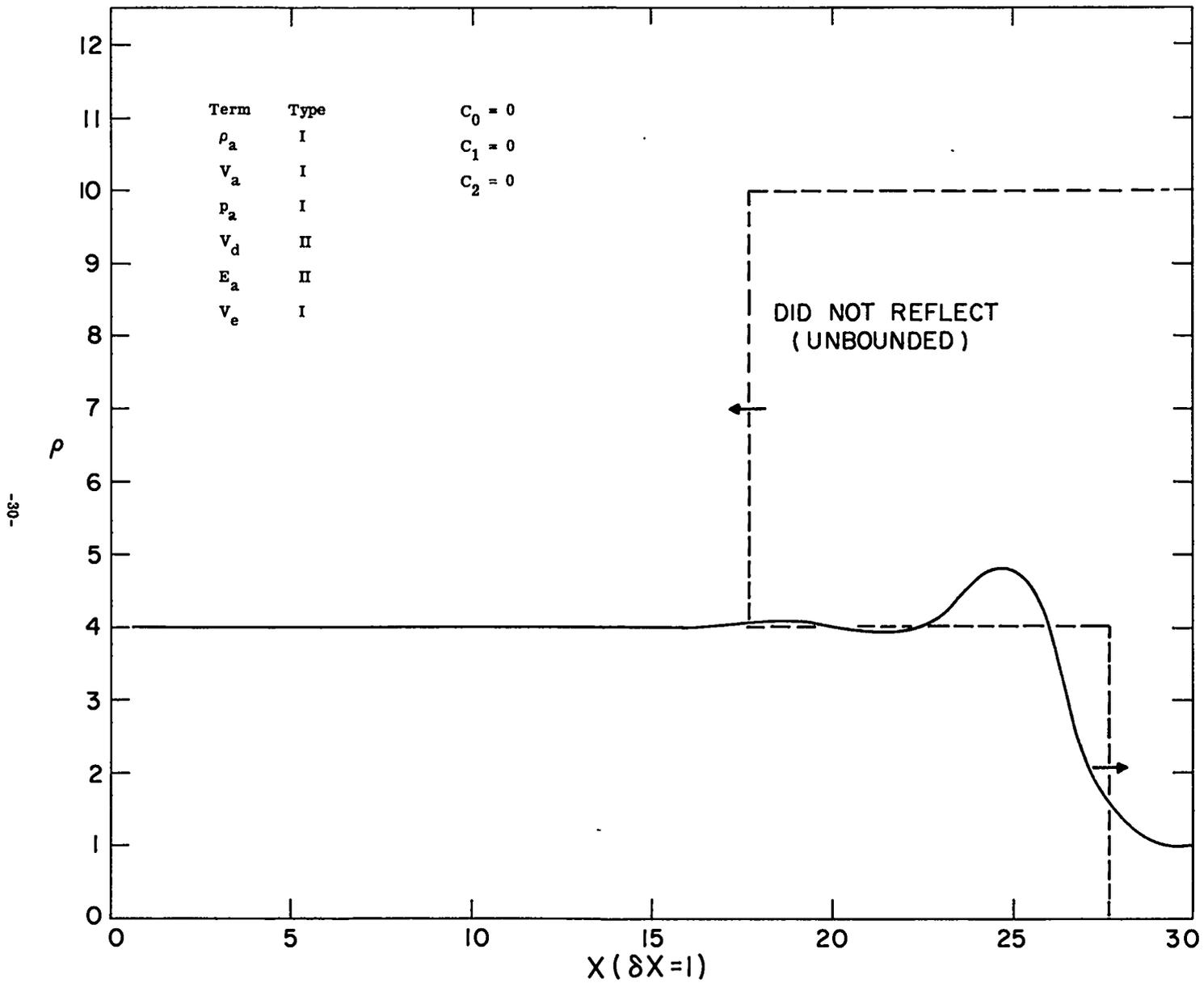
Figure 11

Figure 12

Figure 13

Term	Type
ρ_a	I
V_a	IV
p_a	I
V_d	II
E_a	II
V_e	I

$C_0 = 0$

$C_1 = 0.5, \; \sigma_{LO}$

$C_2 = 0.01, \; H_{j+\frac{1}{2}} = \dfrac{\rho_j + \rho_{j+1}}{2b}$
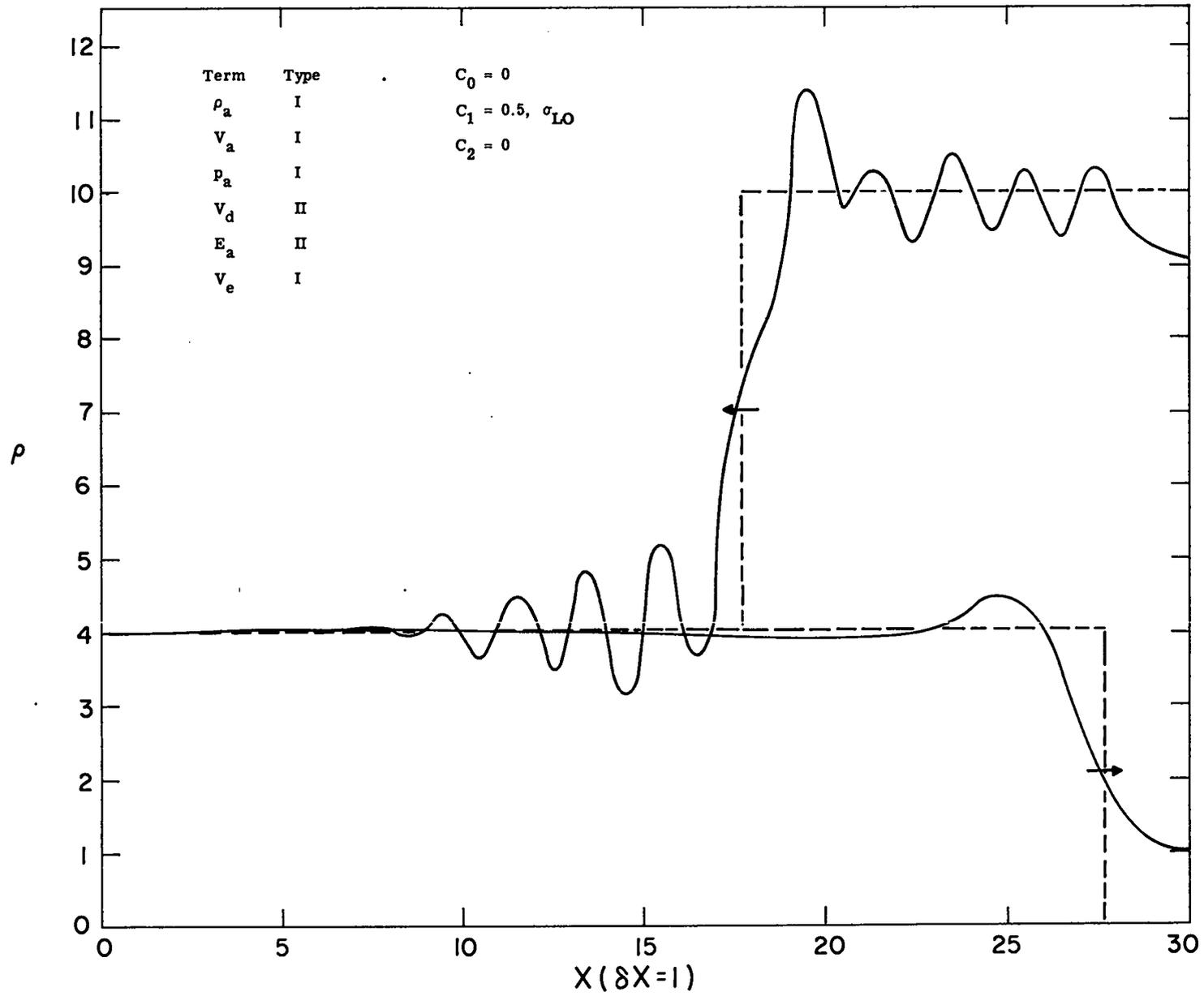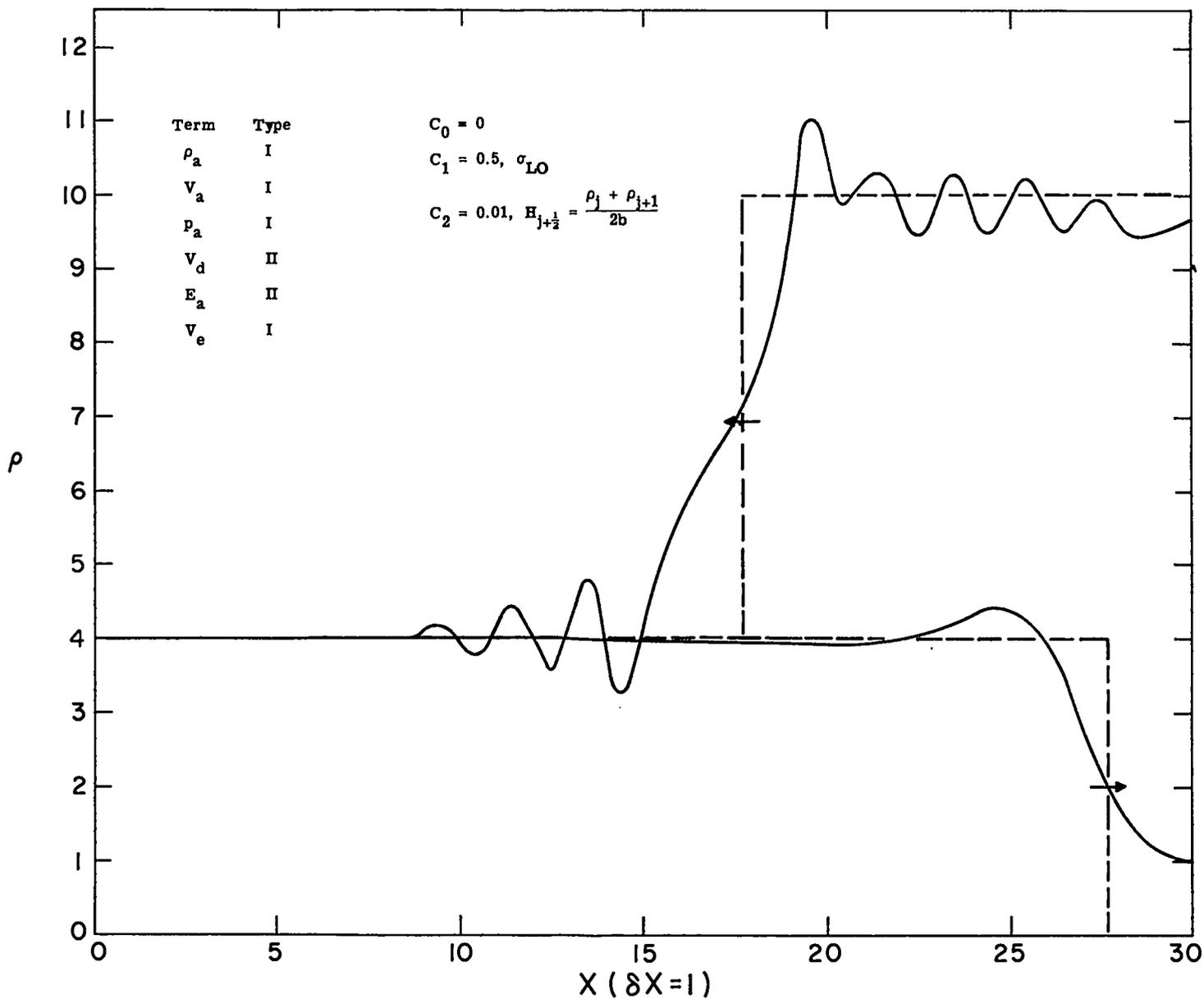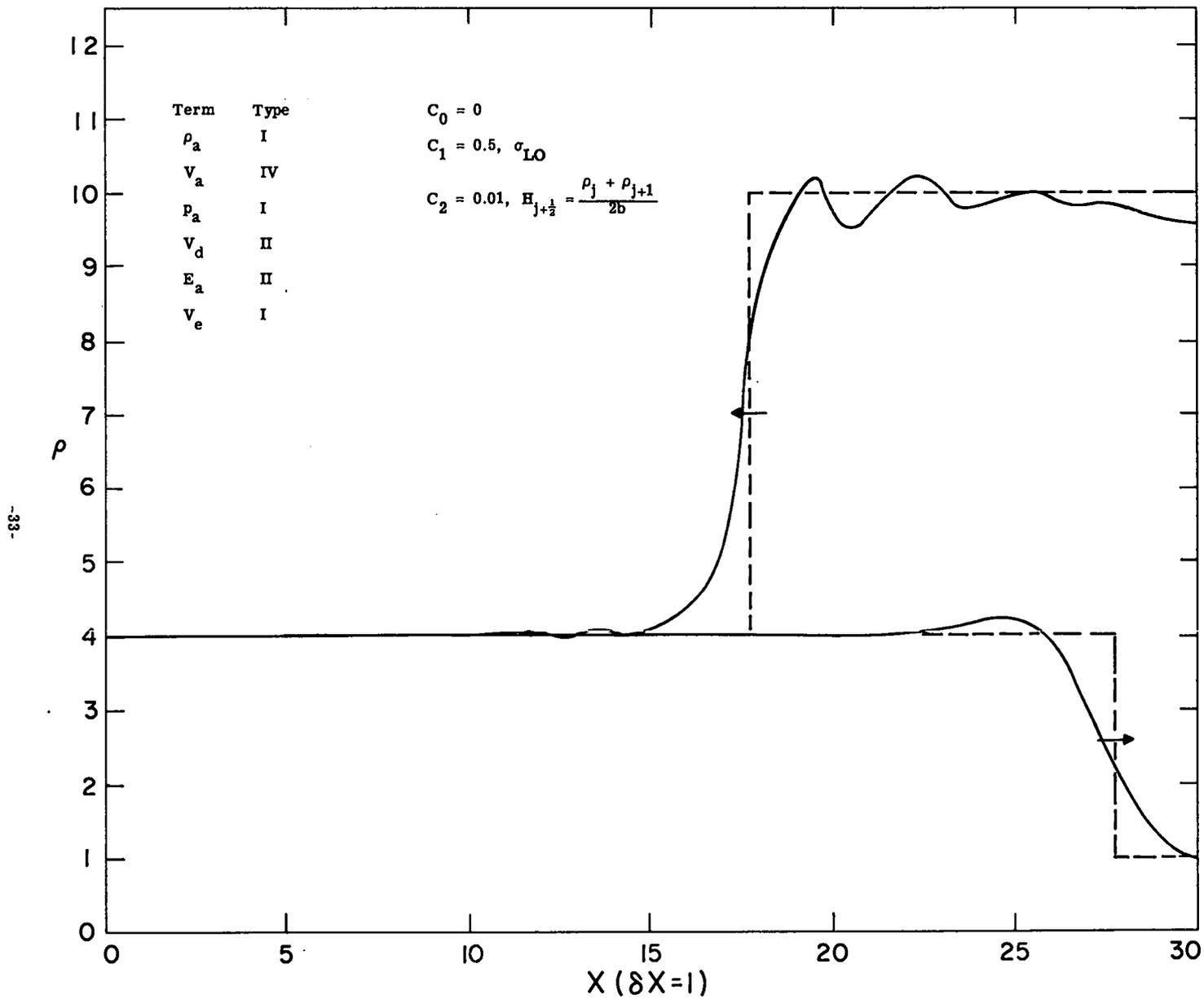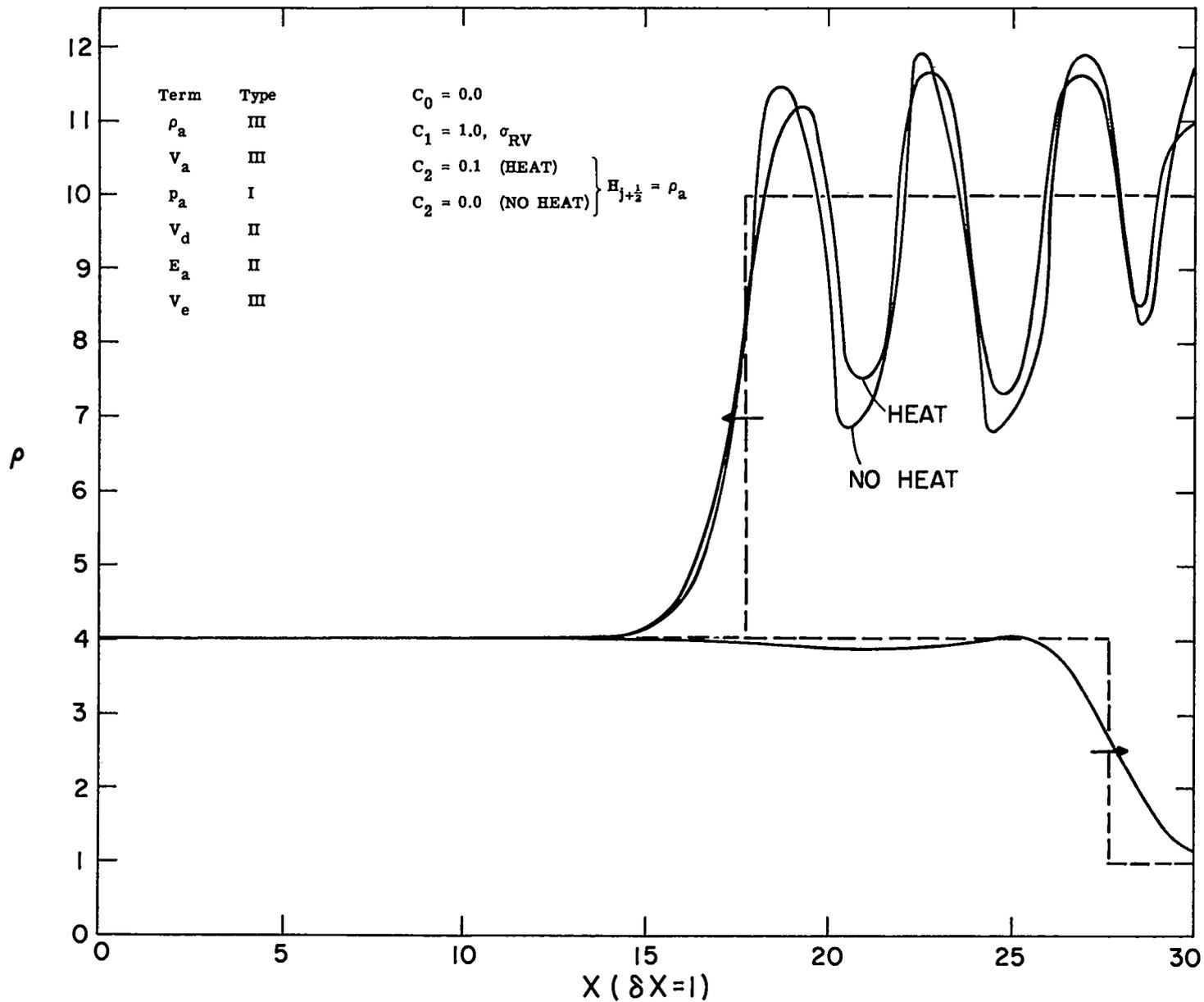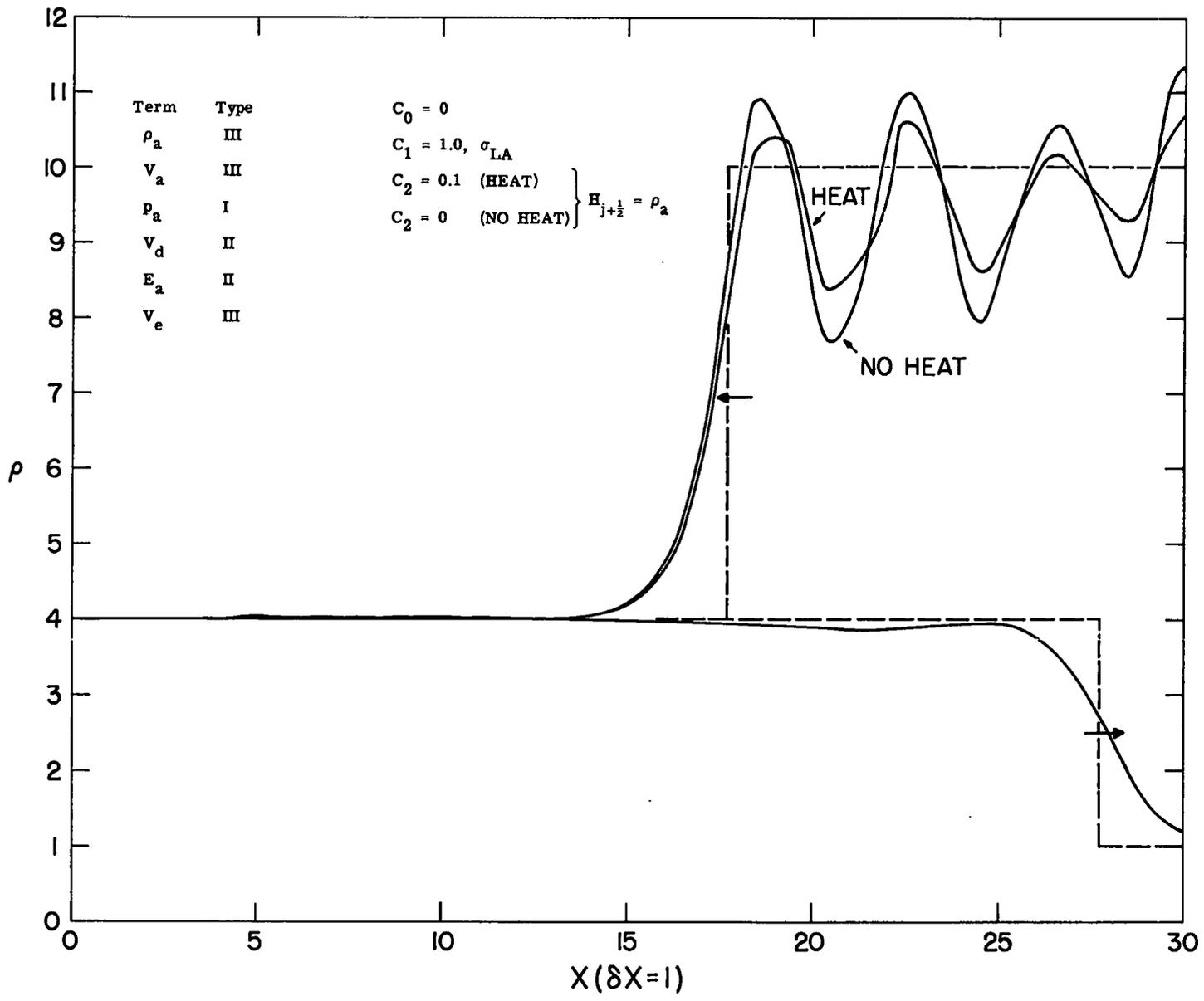
Figure 14

Figure 15

Figure 16
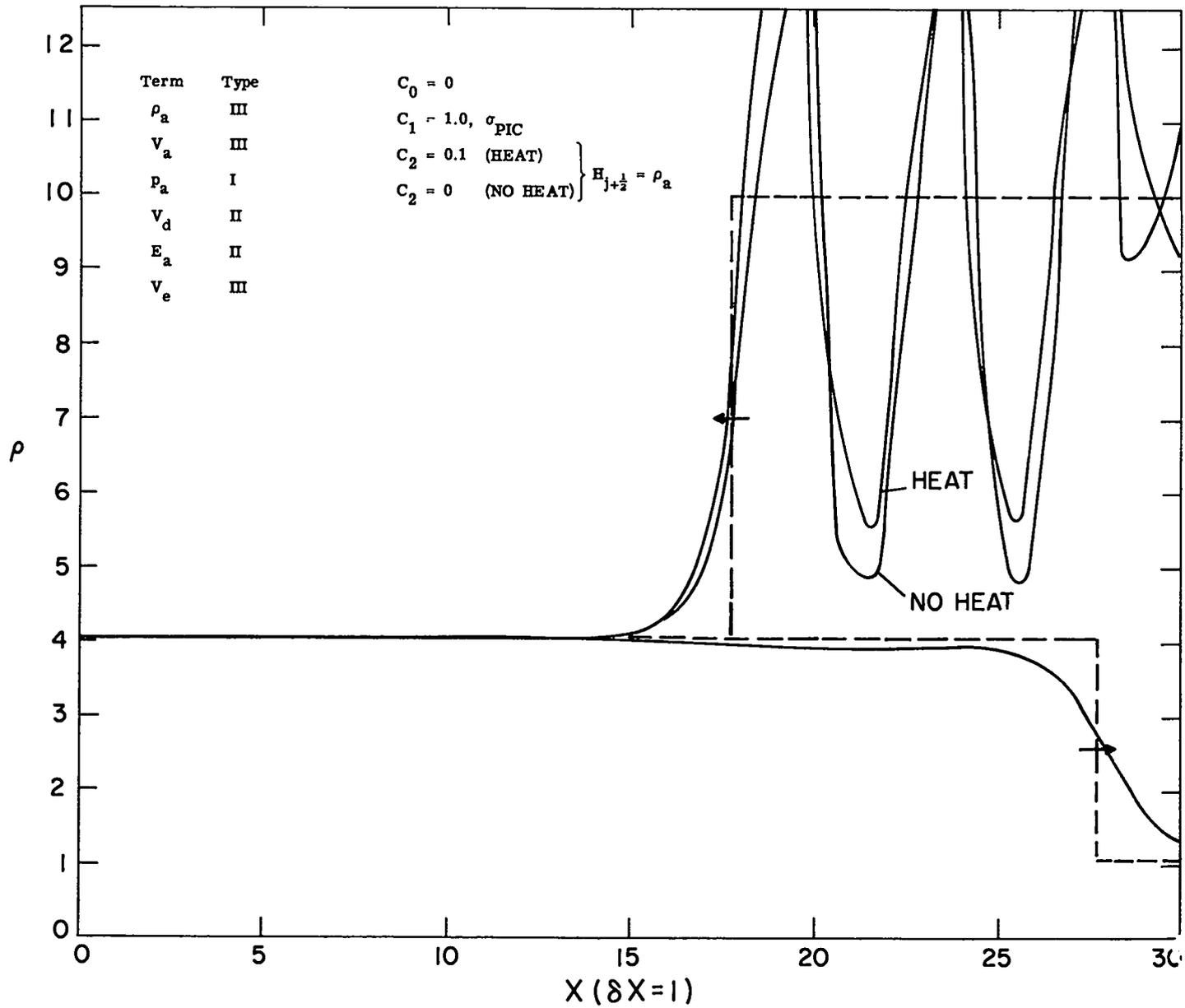
Figure 17
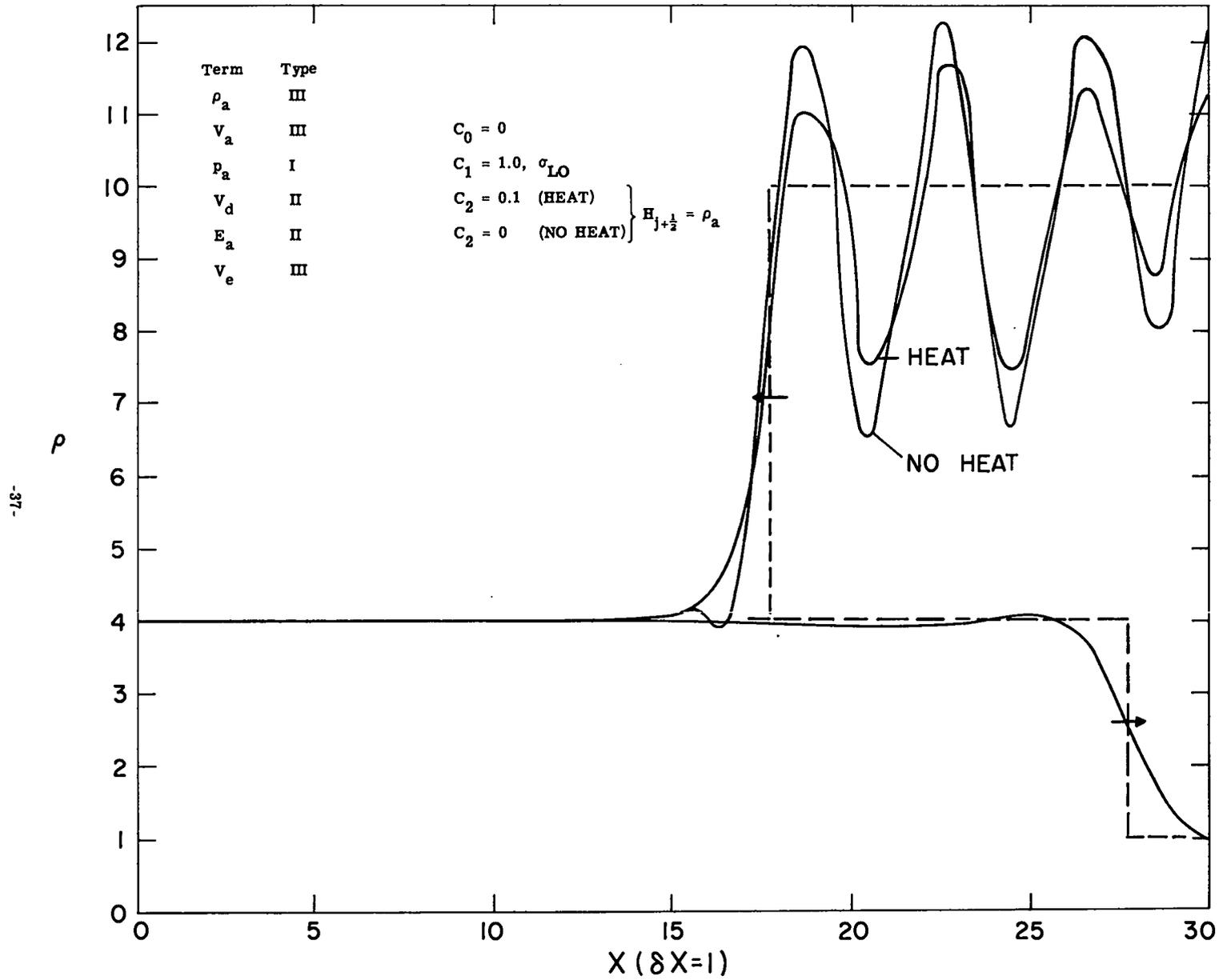
Figure 18
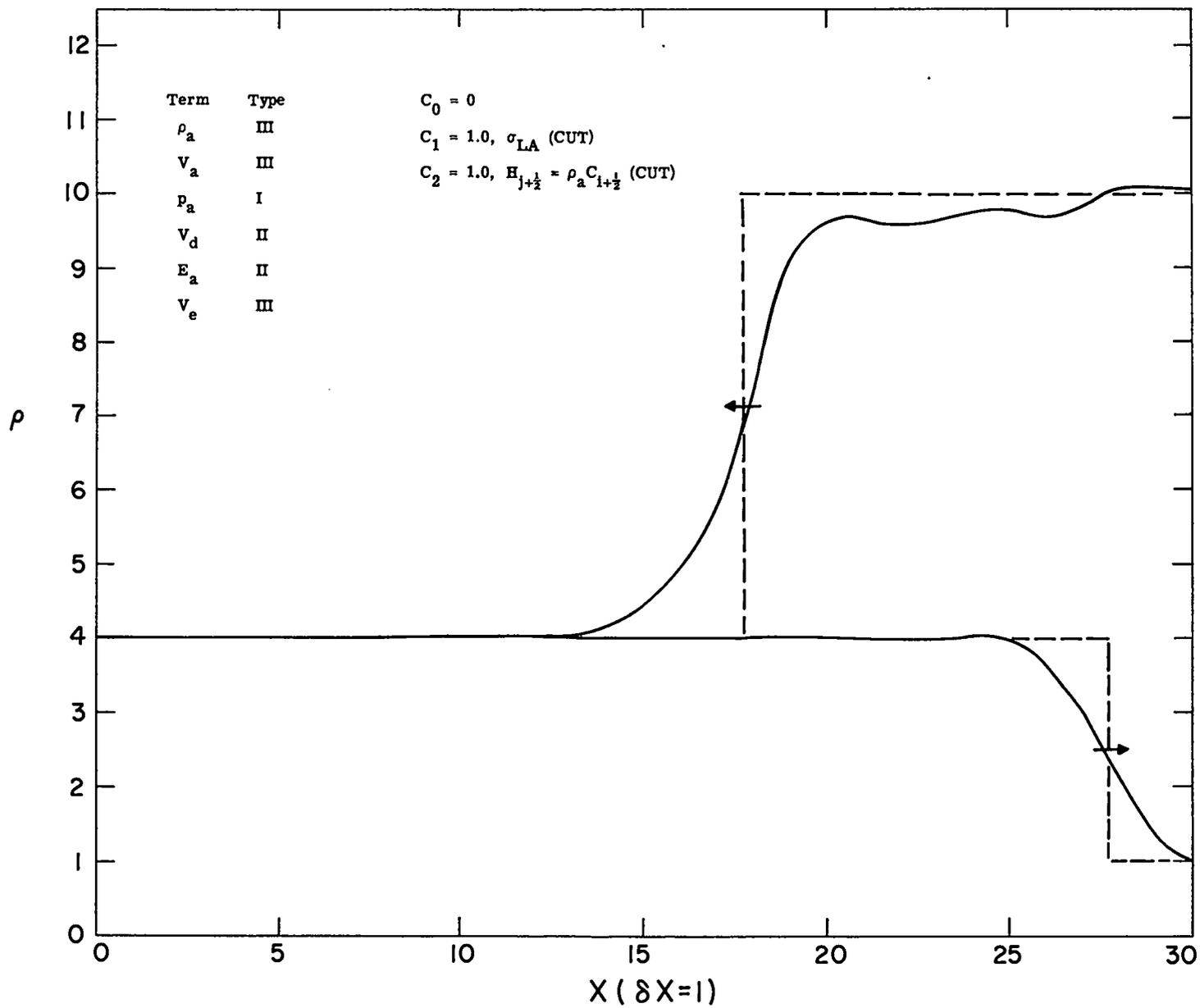
Figure 19
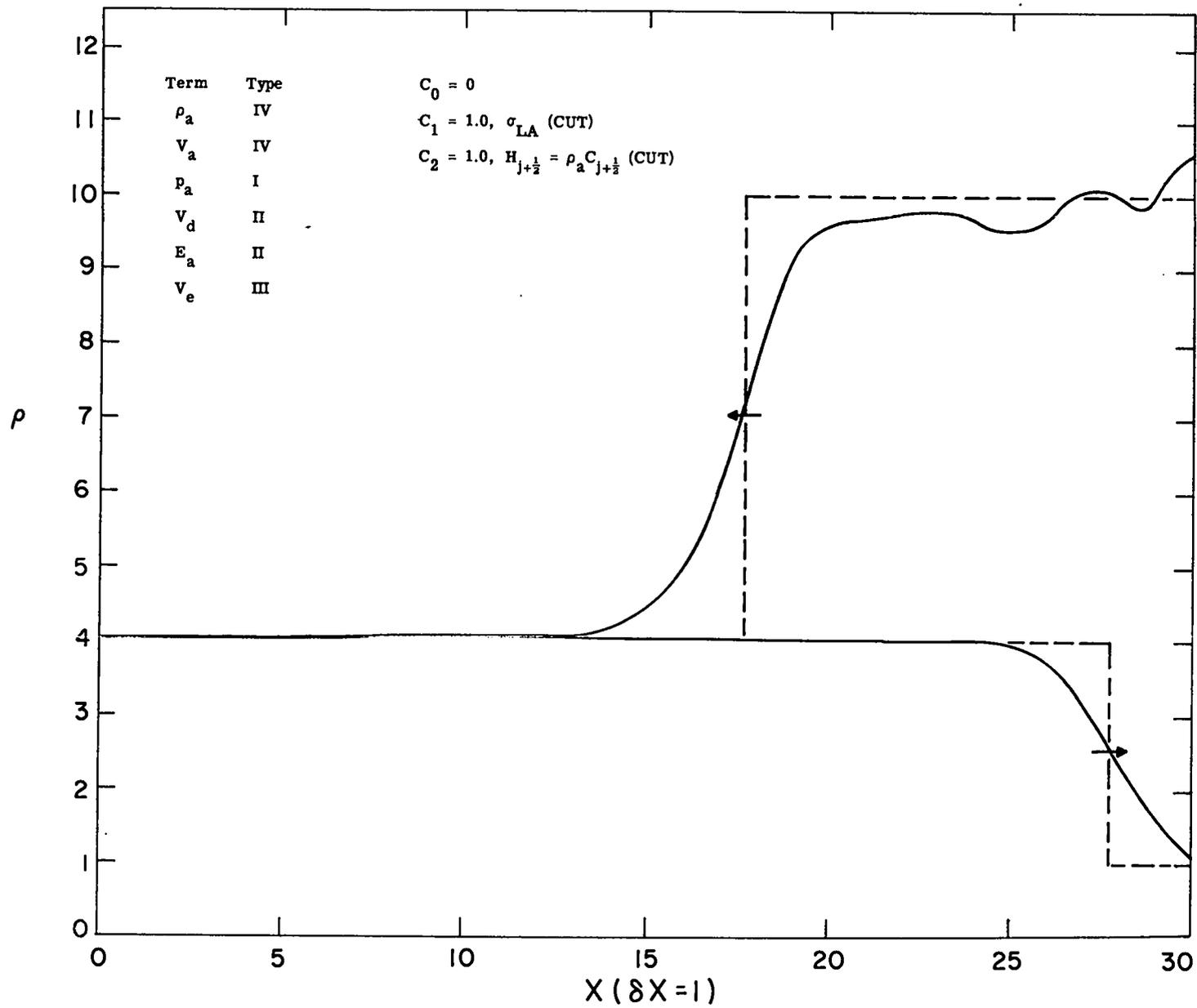
Figure 20
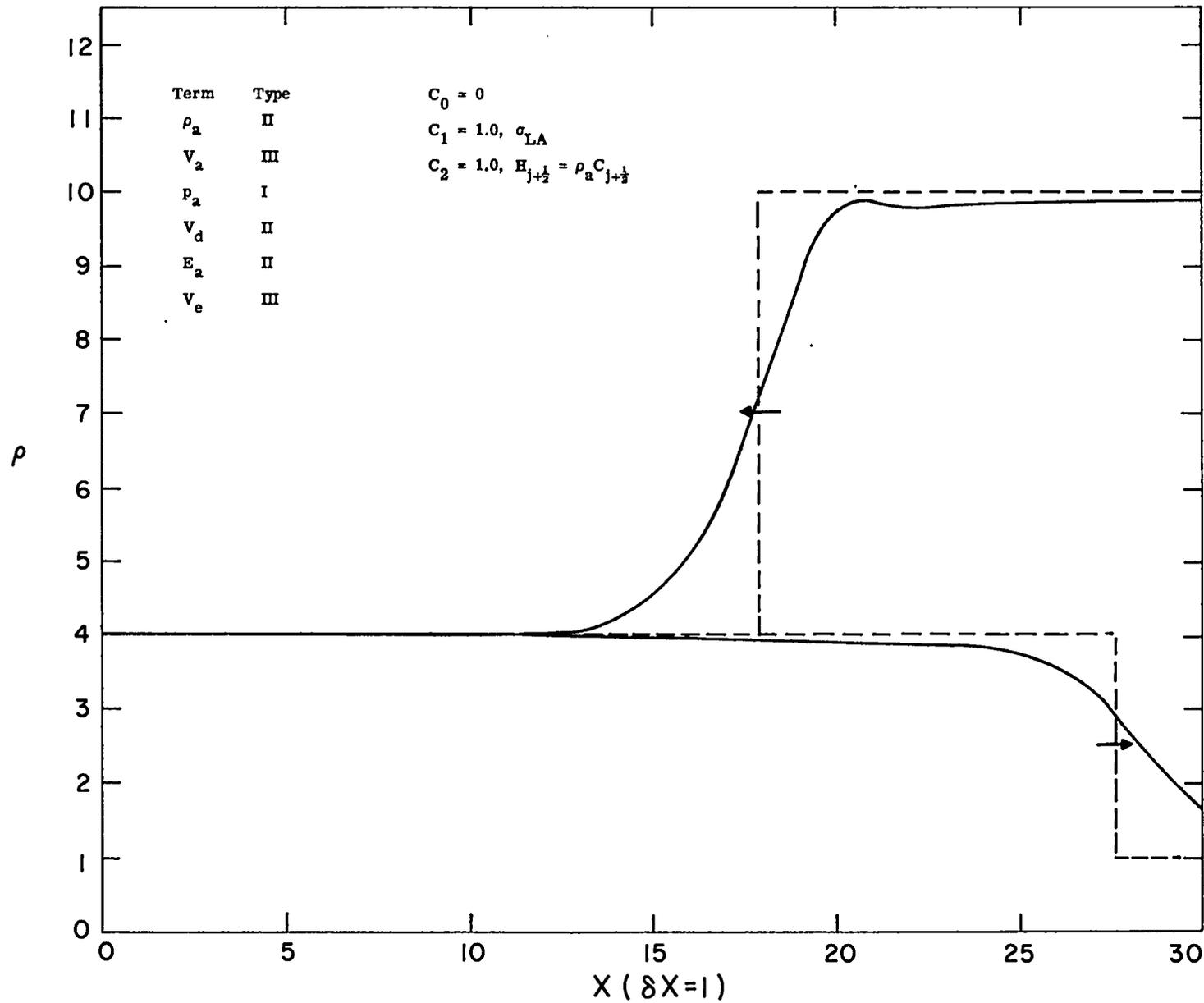
Figure 21

Figure 22

Figure 23

Term	Type
ρ_a	III
V_a	III
p_a	I
V_d	II
E_a	II
V_e	III

$C_0 = 0$

$C_1 = 1.0,\ \sigma_{RV}$

$C_2 = 1.0,\ H_{j+\frac{1}{2}} = \rho_a C_{j+\frac{1}{2}}$

ρ

$X\ (\delta X = 1)$
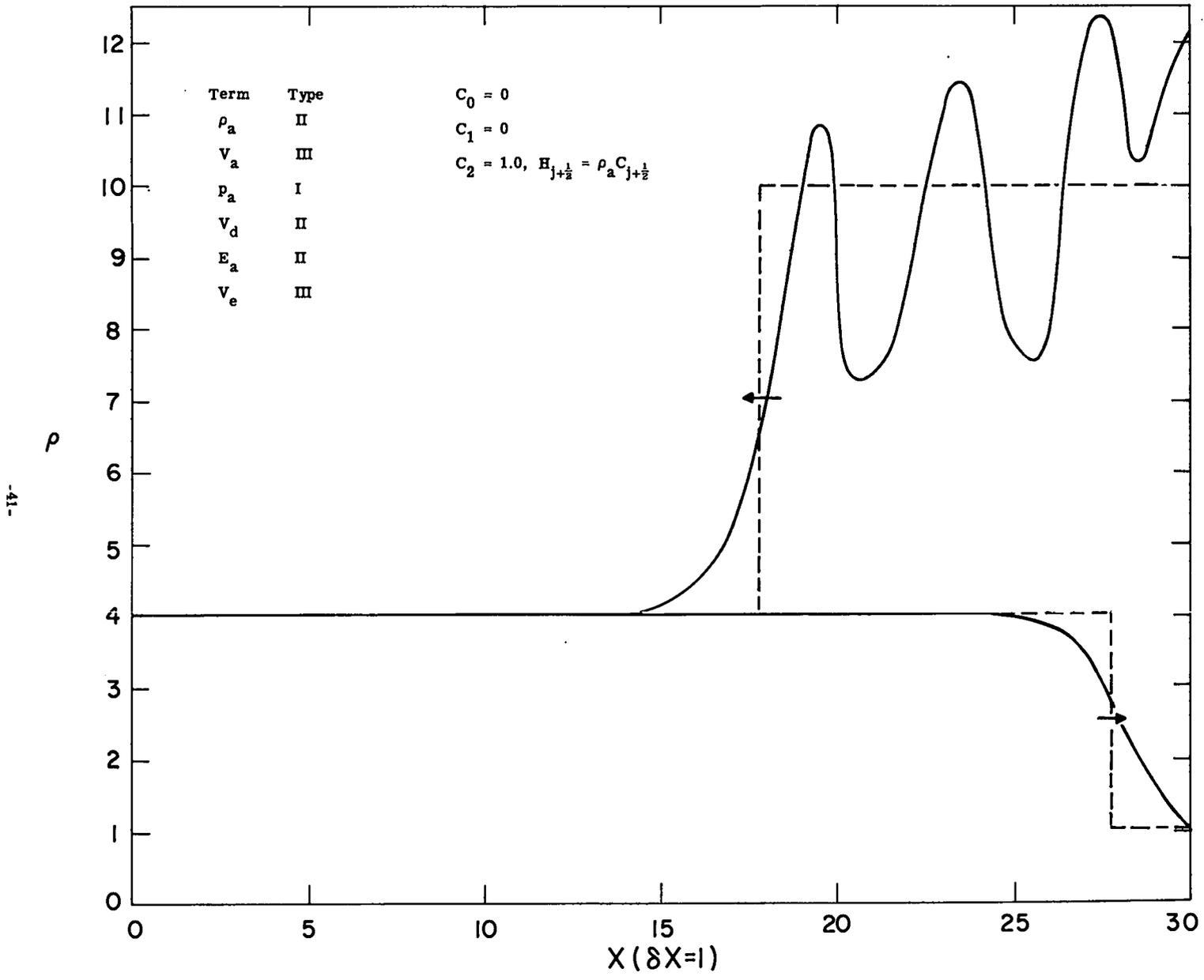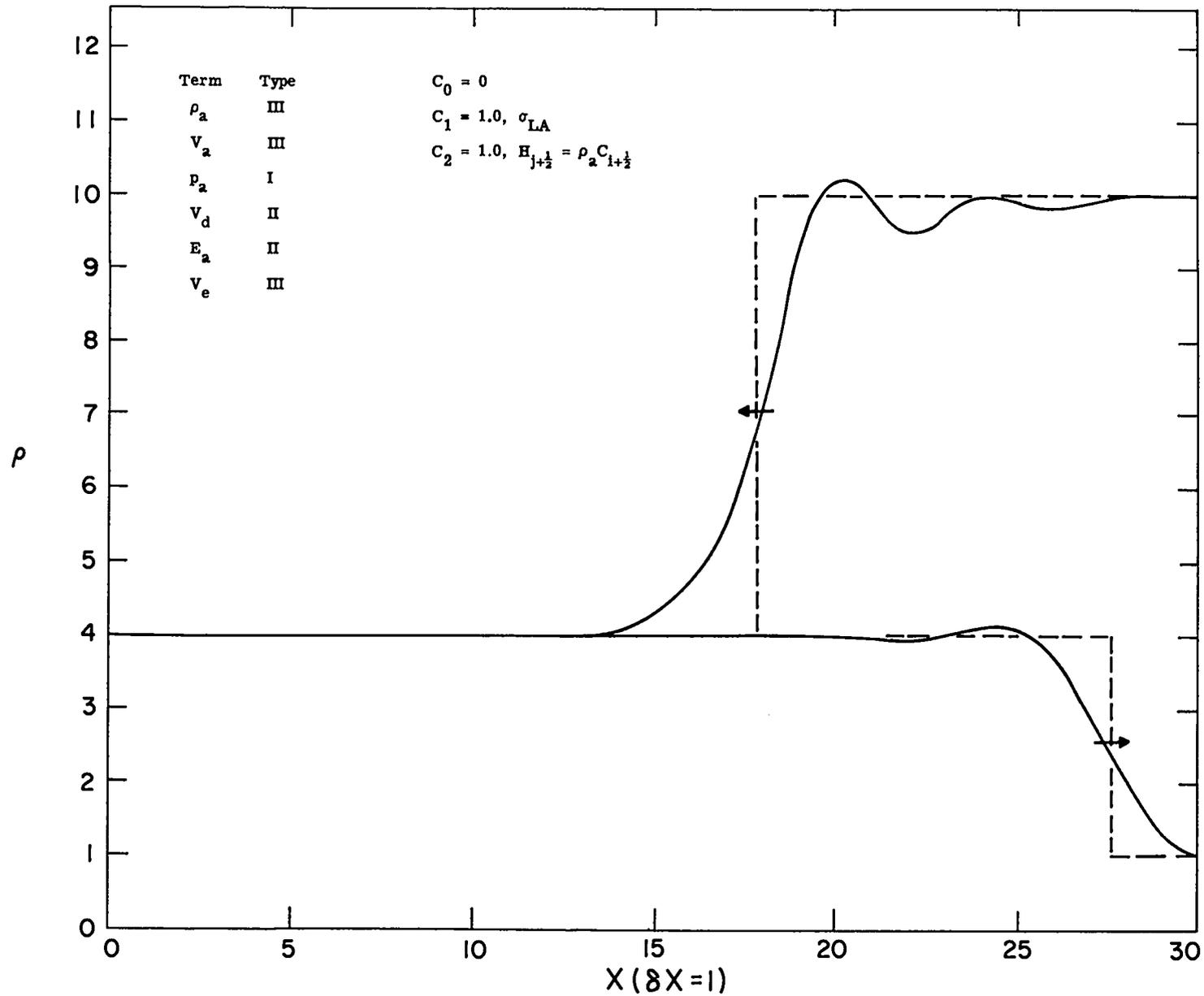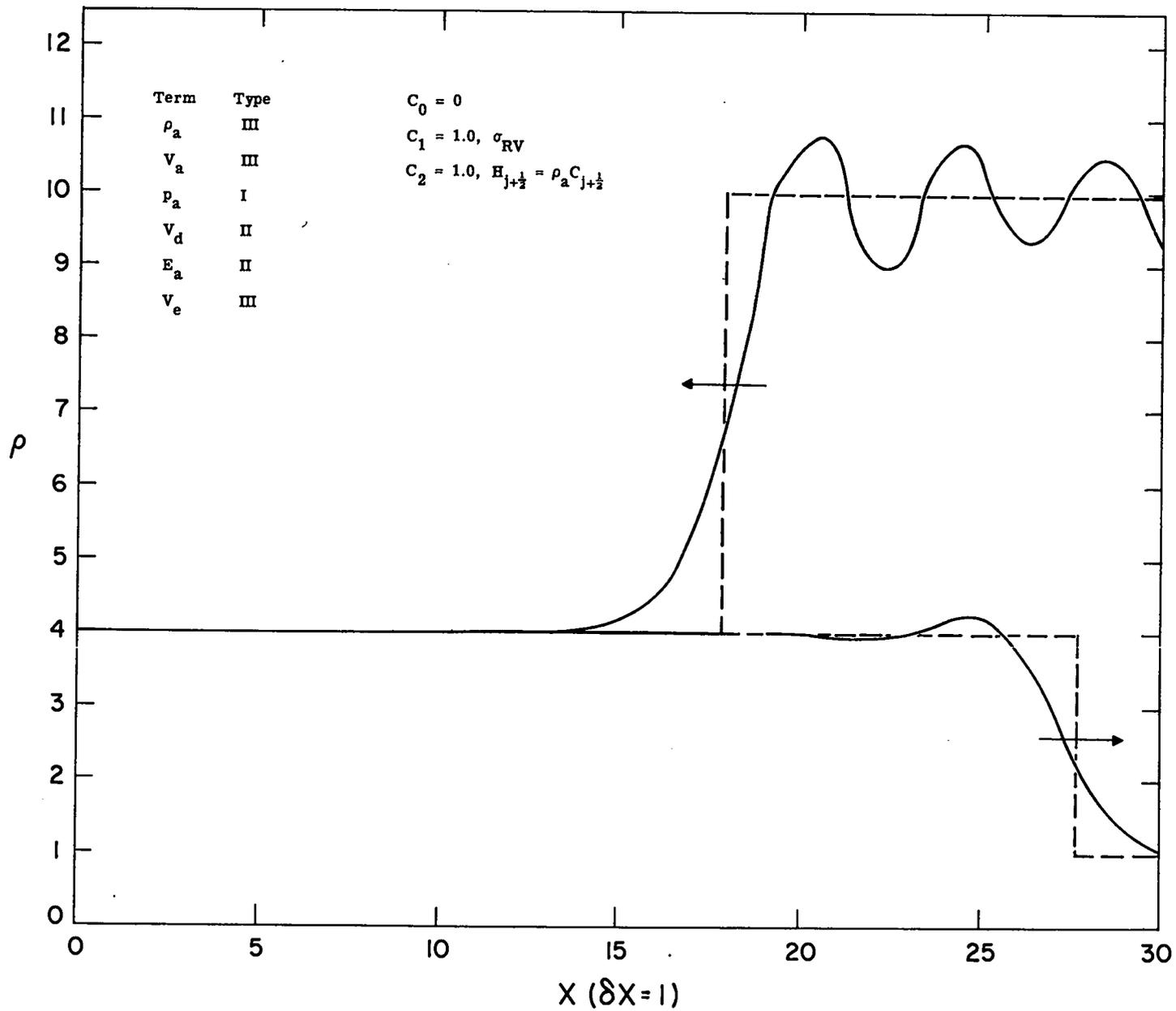
Figure 24

Figure 25

Figure 26

Figure 27

As Fig. 27 except:
Material Velocity
at left input is 0.5

ρ

$X(\delta X=1)$

Figure 28

-47-

As Fig. 28 except:

ρ_a and V_a are Type IV

ρ

X (δX =1)
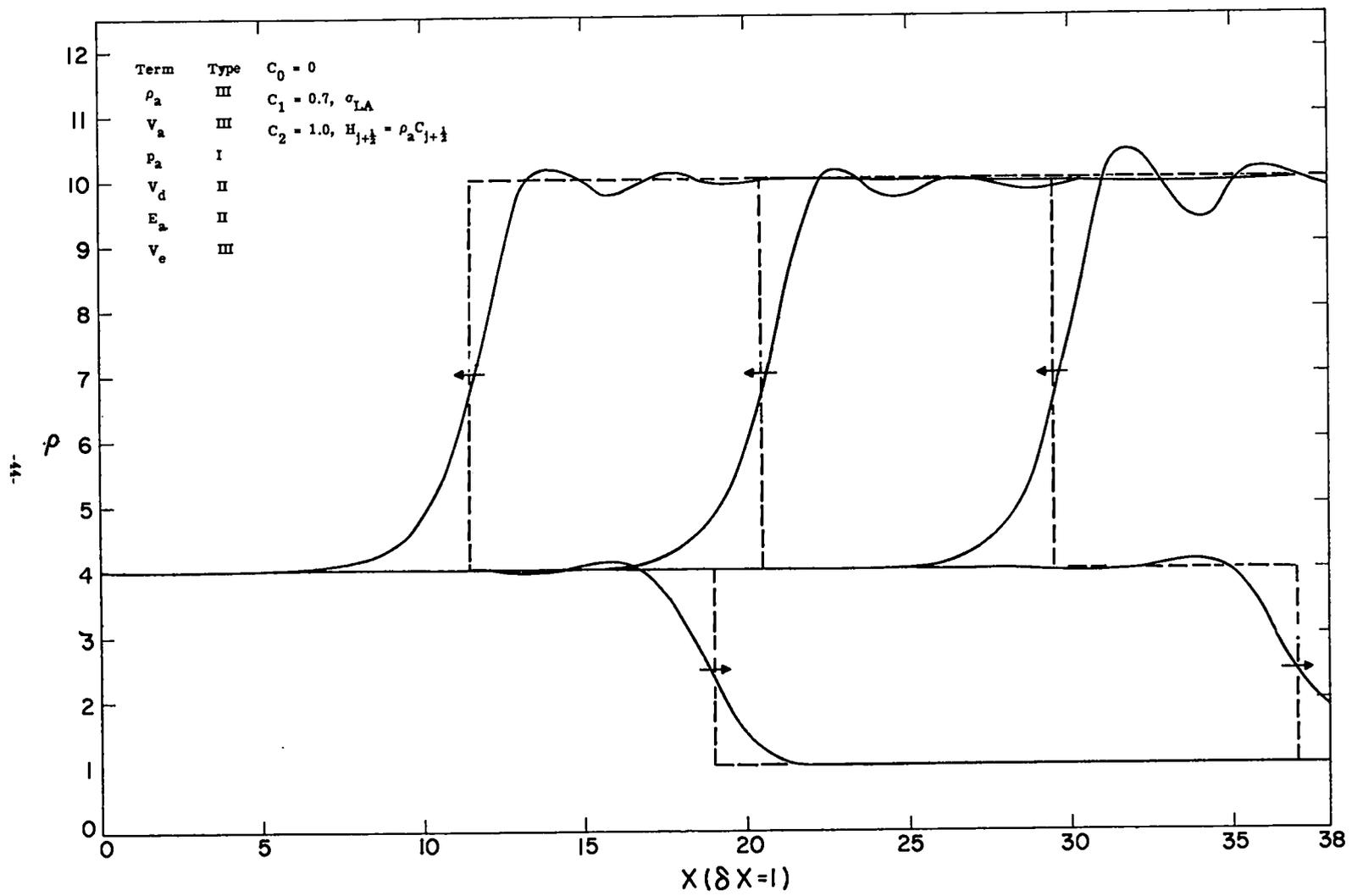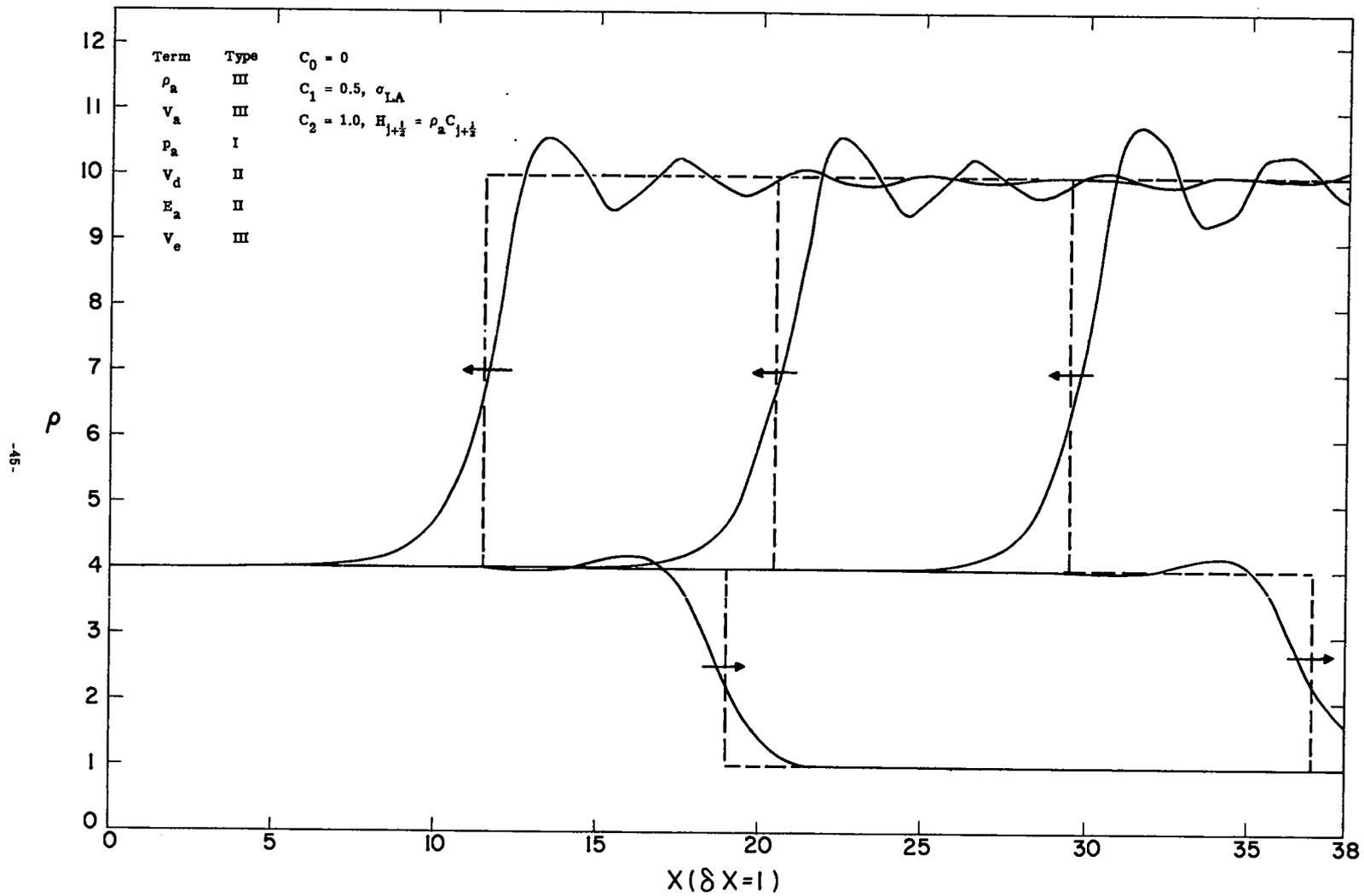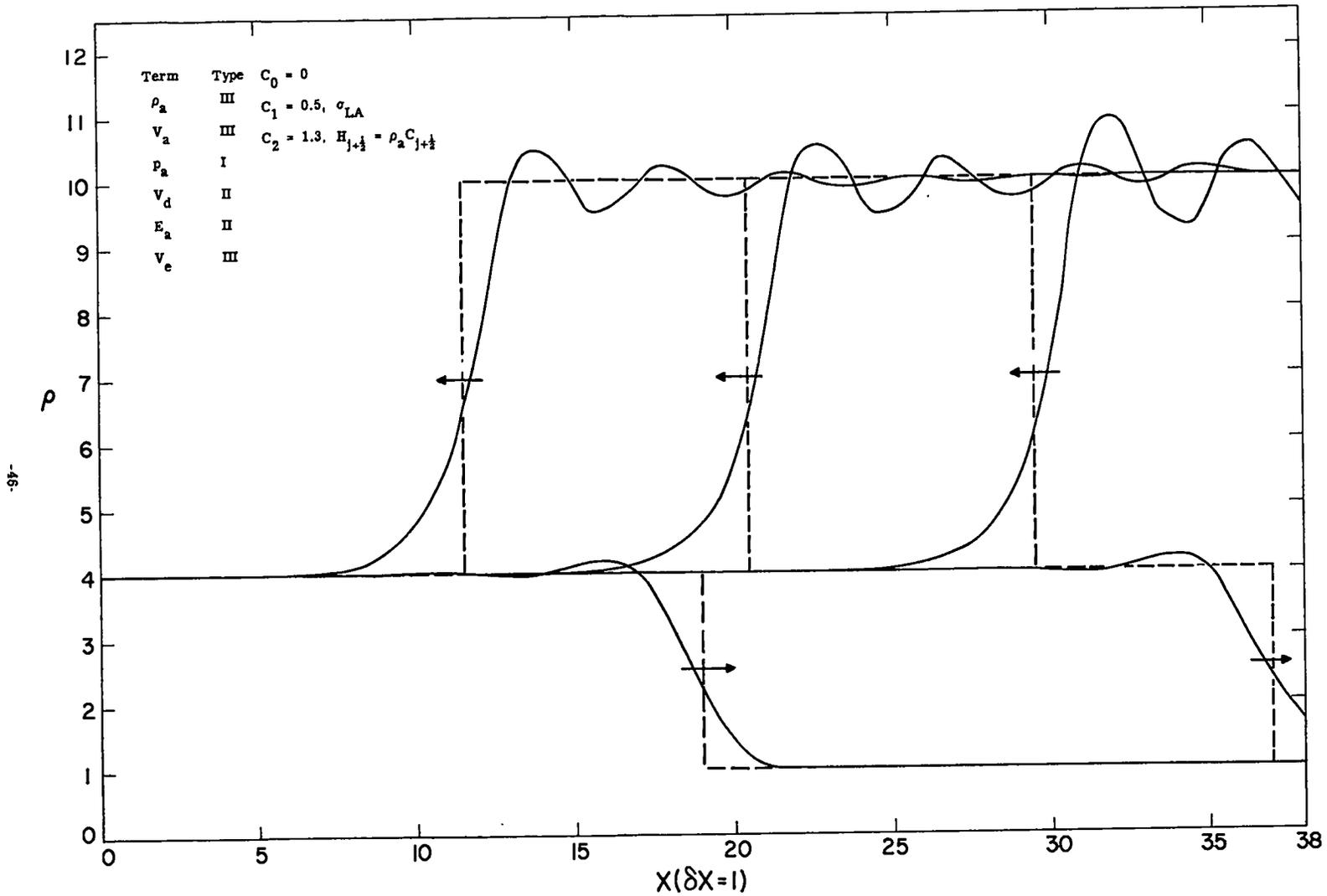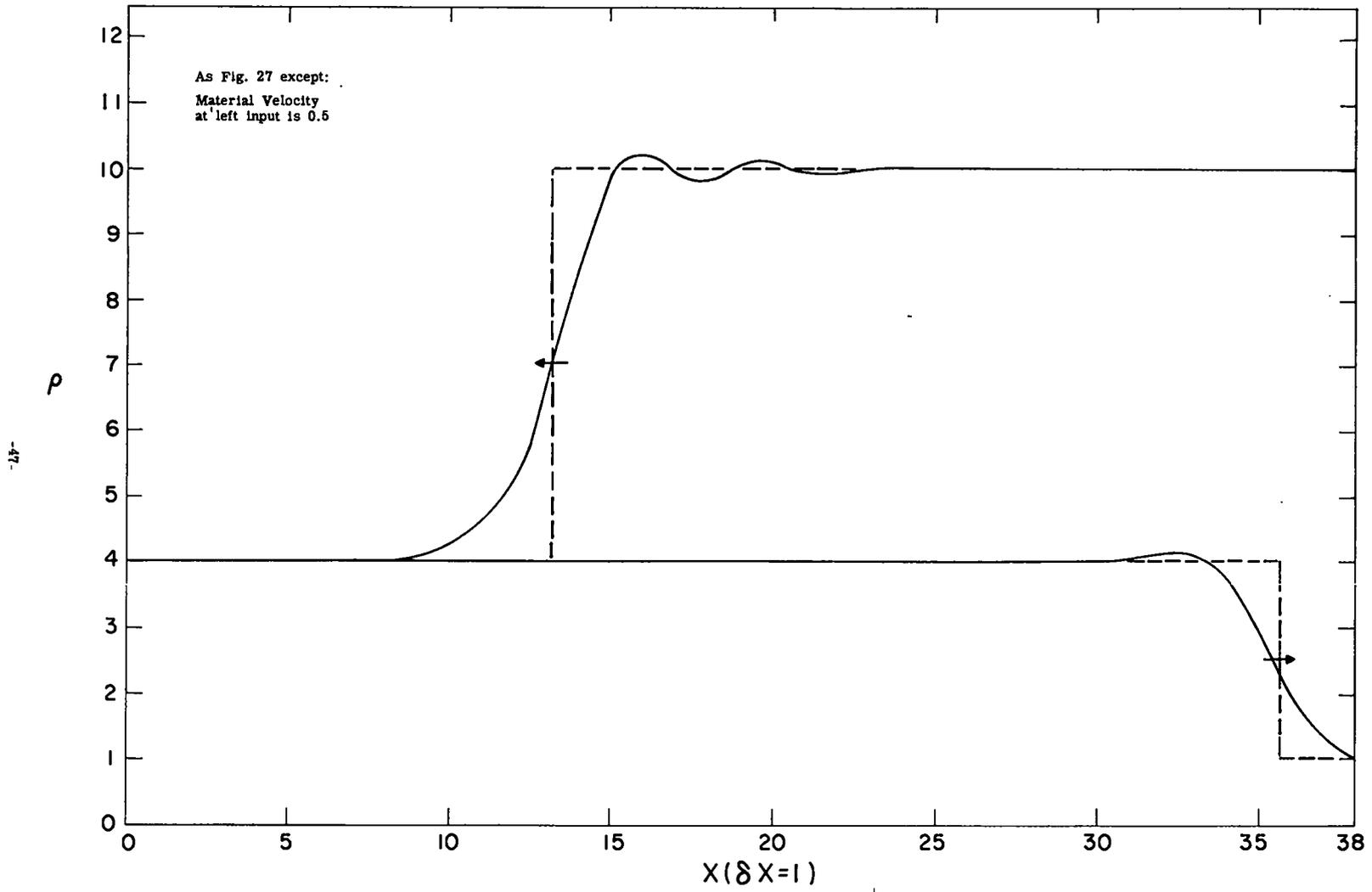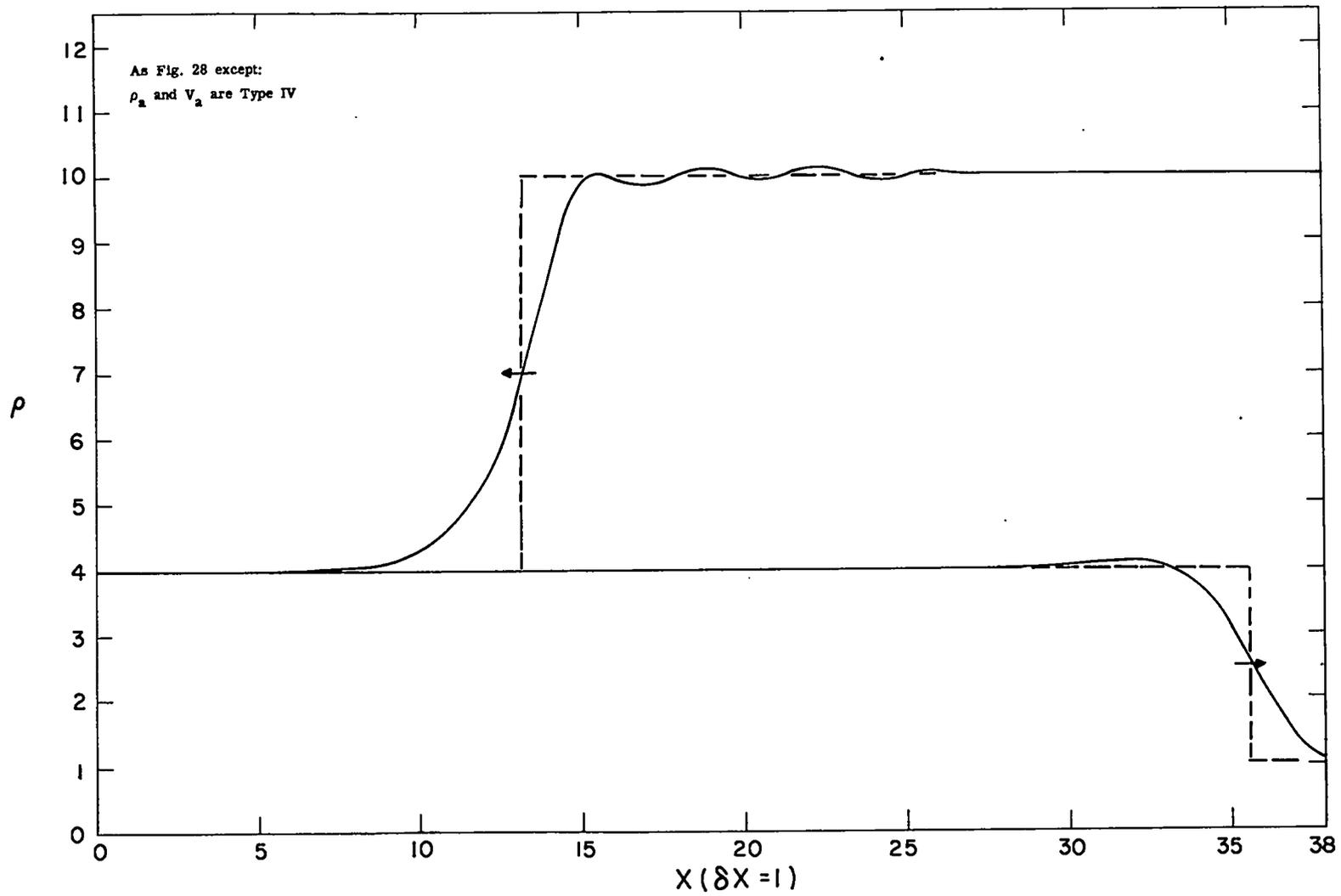
Figure 29

$C_2 \neq 0$, was <u>cut off</u> by the same criterion on the velocity gradient. The explicit mass diffusion term, characterized by $C_0 \neq 0$, was <u>cut off</u> if it was negative. If the word "cut" does not appear after the term characterized by C_0, C_1, or C_2, then the corresponding term was not <u>cut off</u>. The theoretical piston problem should have no rarefactions, but since the machine calculations give oscillations, the use of <u>cut off</u> would give different results for machine calculations. The time at which the various curves are plotted may be calculated (if desired) by knowing the shock velocity (4/3) and reflected shock velocity (2/3) in combination with the plotted position of the appropriate straight line theoretical solutions.

Figures 2 through 6 show some results for the case when ρ_a, V_a, P_a, etc. are each differenced by Type I differencing, i.e., no low order diffusion effects are introduced due to differencing. The density in Figure 2 is plotted at two times to show that the oscillations do not grow and though the calculated shock lags the theoretical shock, the shock speed is correct. The fact that the shock speed is correct in all the piston problems presented seems to be the result of the conservative differencing form and not the differencing types. Throughout, we have taken the shock front position at which the density has a value halfway between value preceding and the value behind the shock front. In Figure 2 the shock is late by about two cells because of an initial delay. The lateness or earliness of the shock front is dependent on the type differencing used. Figures 2 and 3 used the Richtmyer-von Neumann viscosity with the magnitude (C_1)

differing by a factor of six. Figures 3a and 3b show the shock before and after reflection. E and p of the reflected shock are plotted to show that the oscillations in ρ and Θ are out of phase with each other. This phase relation suggested the type mass diffusion coefficient selected in Figure 5. Figure 5 shows, in an extreme case, the effects of mass diffusion on the reflected shock density. Here the density is low by about 15%. Figure 6 shows about the best results that were obtained for the reflected shock from all Type I differencing. Similar results could be obtained by using the Landshoff viscosity. As expected, the results in the reflected shock region (stagnation region) were not nearly as good when a Richtmyer-von Neumann or pic viscosity was used. This is, of course, due to their dependence on velocity rather than temperature. The oscillations in Figure 2 which result from not enough diffusion may also be considered to be the result of not enough entropy change. Similarly, Figure 5 would appear to show too much entropy change.

Figures 7 through 29 show the results for the various diffusion effects introduced by combinations of the four types of differencing with explicit heat conduction and viscosity. By unbounded in Figure 11 we mean that the oscillations in the reflected shock were greater than the capacity of the machine, i.e., greater than about $10^{\pm 38}$. The incident shock is fairly good in most of the situations shown. The worst cases shown occur when ρ_a is differenced as Types I or II for certain cases (Figures 8, 9, 10, 11, 12, 13, and 21). Thus, finding the correct scheme for producing a good reflected shock appears as the more

difficult problem. For the reflected shock (stagnation) region, one can
see from the curves that one needs both an explicit heat conduction and
an explicit viscosity to produce the proper entropy change. We will now
discuss the preferred scheme, along with the reasons for its selection,
and mention some possible modifications. Thus, the curves will not be
discussed individually but will be referred to at various times to il-
lustrate conclusions.

We wish to find the best scheme for evaluating the terms in Eqs. (11),
(12), and (13). We have already seen that we should take $p_a = p_b$ and $\rho_a V_a$
$= \rho_b V_b = \rho_c V_c$. We calculate p_a by Type I differencing. We are left with
the problem of selecting ρ_a, V_a, V_d, E_a, V_e, and the three explicit dif-
fusion terms. We will give V_d and E_a Type II differencing for several
reasons. First, Type II takes the least machine time of the four types
considered. Second, the equations need diffusion effects for stability.
Third, these diffusion effects are of the right order of magnitude for
shocks and do not result in excessive spreading of shocks (see Figures 7
through 29). We generally let $V_e = V_a$, since V_a will have already been
calculated, though calculations show that its selection is not very im-
portant. We are now left with the choice of the diffusion terms and the
mass flow $(\rho_a V_a)$ as the major problem. If a stagnation region or region
of low velocity (where the pic type viscosity, introduced by selecting
V_d as Type II, goes to zero) is to be present in a problem, then one
should have an explicit viscosity and heat conduction term. The best

type viscosity is then that given by Landshoff, as may be seen from Figures 15, 16, 17, 18, 23, and 24. If one really worries about machine time and if one can approximate the stagnation region sound speed, the viscosity σ_{LO} may be used. The best heat conduction coefficient found in the present work is given by $H_{j+1/2} = \rho_a C_{j+1/2}$ (see Figures 19 through 29). Thus, if σ_{LA} were used, the values for $H_{j+1/2}$ would have already been calculated. It now seems that a good value for $D_{j+1/2}$ might also be given by the product of density and sound speed, though this was not tried. Mass diffusion (see Figures 5, 8, 9, 10, and 21) terms left the density too low in the reflected shock in all cases where the oscillations were reduced with terms characterized by $C_1 \neq 0$ and $C_2 \neq 0$. Therefore, the mass diffusion term is taken out ($C_0 = 0$). Figures 2, 3, 4, 6, 11, 12, and 13 show clearly the results of differencing ρ_a as Type I. Thus, if stagnation regions are to be present, ρ_a and V_a should be differenced as Type III or IV. The above diffusion terms make the density continuous in any given material. This fact, plus the fact that one wishes to move the mass as accurately as possible through the mesh, makes the author prefer Type III differencing for ρ_a and V_a. Type IV takes less machine time and appears nearly as good (see Figures 28 and 29) for this problem. If there is to be no stagnation region, then the results given by Figure 7 appear to be the simplest and fastest method of differencing for the piston problem. To summarize, Figure 19 gives what we call the best scheme (see also Figures 23, 25, 26, and 27) if the problem at hand is to have regions where the Mach number is less than unity. The terms characterized

by $C_1 \neq 0$ and $C_2 \neq 0$ may be set to zero in a region of high Mach number to avoid excessive spreading of shocks. However, this was not done in any of the test problems of this paper.

We will now present the results of the study of the fractured diaphragm problem. The same gas constants as used for the piston problem are used for both materials of the diaphragm problem. The best results obtained are shown in Figure 30. It may be noted that the "best" differencing scheme for the piston problem was used. If Type IV differencing is used for ρ_a and V_a, then one obtains exactly the same curves. If the two explicit diffusion terms are not "cut off," then the rarefaction at its left side is four cells ahead of where it should be instead of the two cells as shown. In each case the ultimate speed was correct. Since the rarefaction wave and the contact discontinuity present the two new difficulties in the diaphragm problem and since the differencing scheme with "cut off" gives the best rarefaction wave, the main problem is the contact discontinuity. The initial values at time zero and the theoretical values are both represented as straight lines (Figure 30).

The contact discontinuity or interface is contained in one cell. Physically, the velocity and pressure are continuous at the contact discontinuity. Thus, a desirable scheme would be to carry one velocity, two temperatures or internal energies, and two densities for the interface cell. Schemes such as this but which carry only one temperature for the interface cell were tried and gave very poor results in
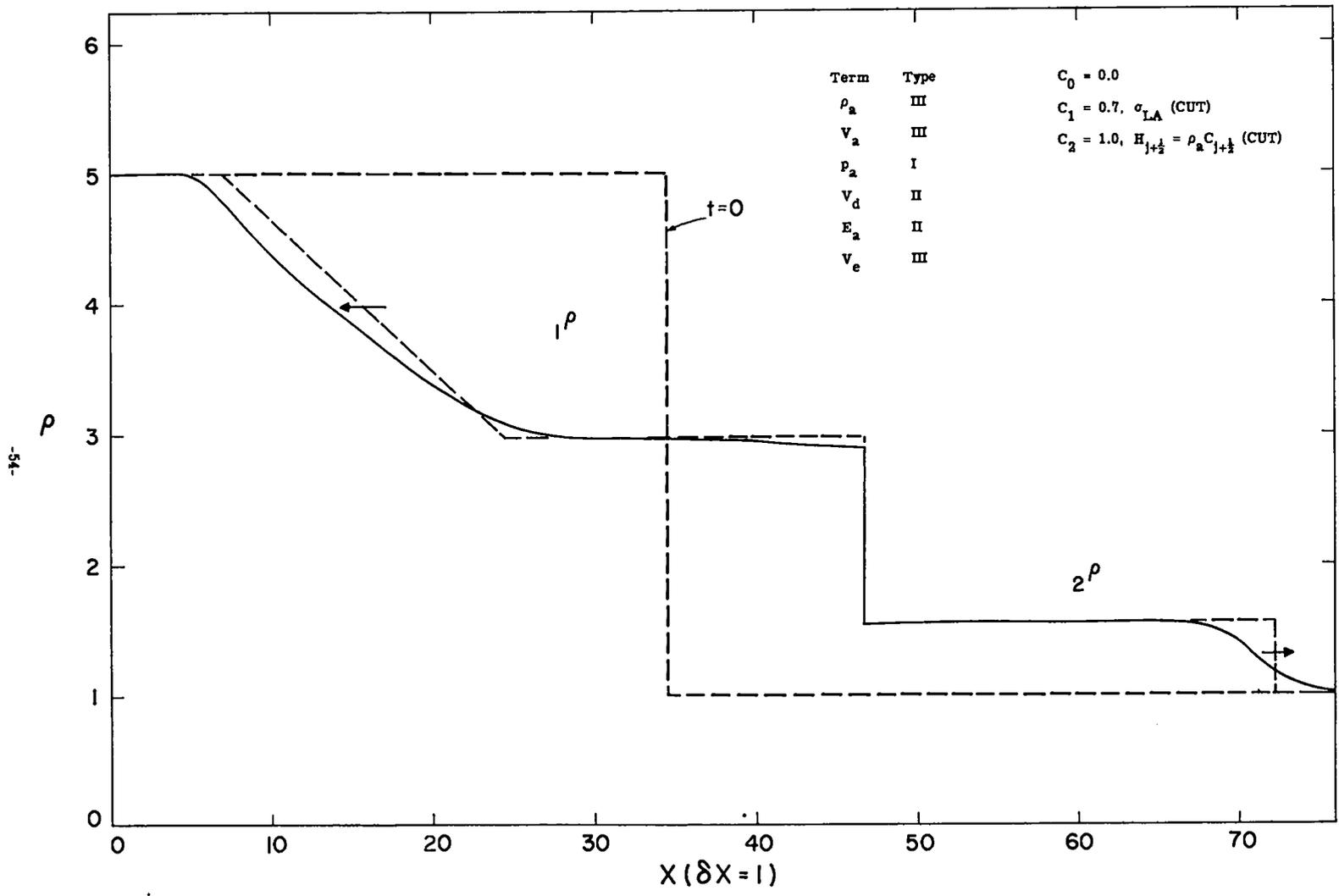
Figure 30A
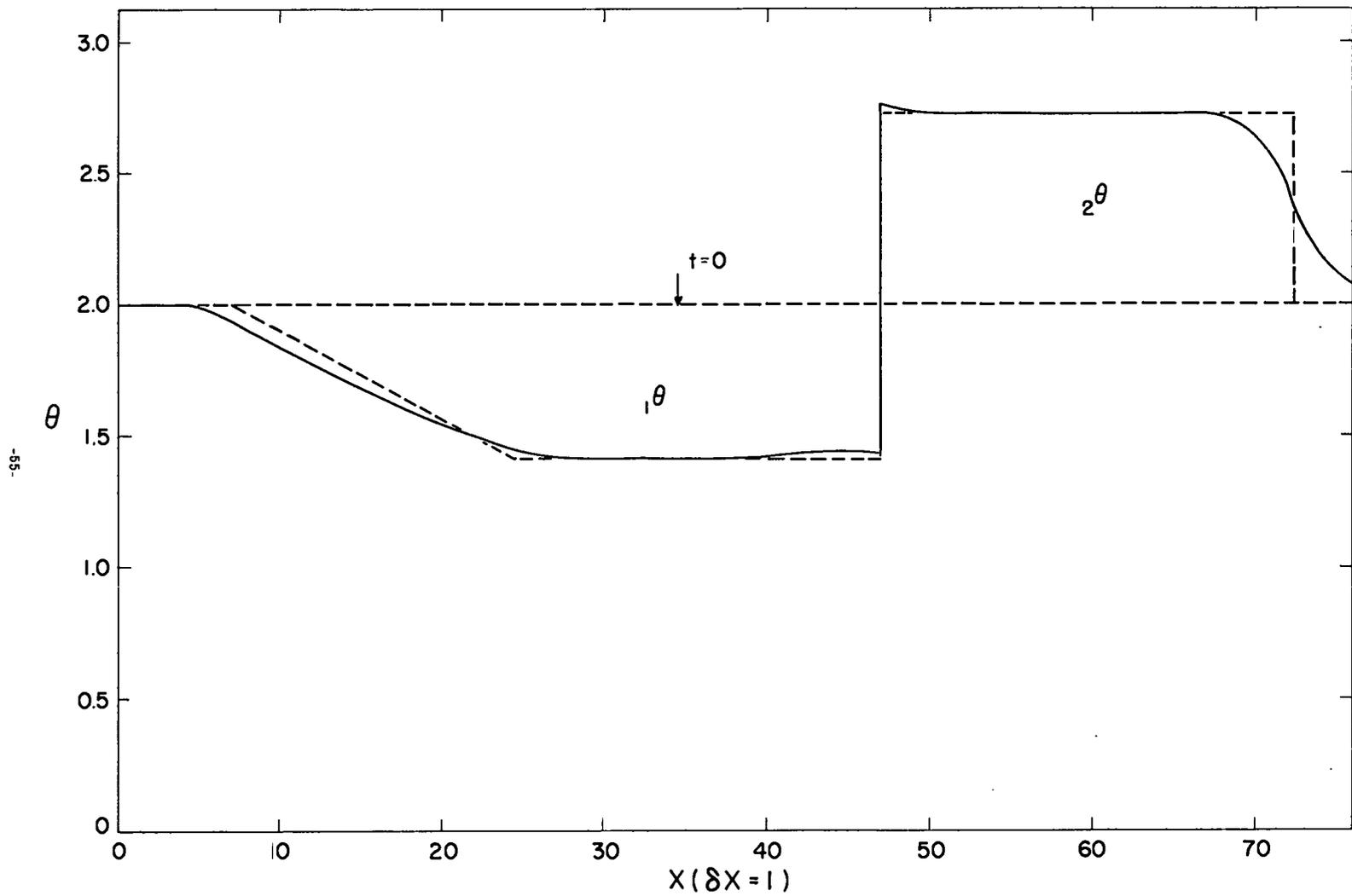
Figure 30B

Figure 30C

the temperature and density curves, because the pressure tends to remain constant. Schemes which carry only one density in the interface cell were not considered, since we did not wish to allow one material to diffuse into another. Call the contact discontinuity cell or interface cell JC. From Figure 31, we see that we must carry the volume of one of the materials in JC. We carry the volume of material one, x_1, and let x_2 be computed by $x_2 = \delta x - x_1$. The problem is then to solve two equations like (4) (one for each material), one equation like (5) (with both materials considered), and two equations like (6) (one for each material) to advance the mesh values in JC to the next time step. After JC and the rest of the mesh have been advanced one time step (the n + 1 calculation), the value of x_1 is advanced one time step. The equations used to advance

Figure 31

the mesh values will not be given at this point but will be given later in more general two-dimensional form for cylindrical coordinates. The conditions which are prescribed to solve Eqs. (4), (5), and (6) in JC are: $(\rho V)_{j+1/2}$ is zero for material one; $(\rho V)_{j-1/2}$ is zero for material two; the pressure in JC is the average of material pressures one and two $\left(p_{JC} = \dfrac{{}_1 p + {}_2 p}{2} \right)$; the total mass must be accelerated in Eq. (5); $(pV)_{j+1/2}$ (the work done by the pressure) is zero for material one; and $(pV)_{j-1/2}$ is zero for material two (see Eqs. (32) and (33)). The terms of Eqs. (11), (12), and (13) are differenced as before except for ρ_a near JC. When considering material one, if the differencing calls for a value of density in a cell beyond the boundary of material one, the value of the density used is that of material one in JC. Similarly, the values for material two densities are extrapolated. Differencing ρ_a as Type II at only the sides of cell JC gave poor results. σ_{LA} is discontinuous at the contact discontinuity so that we found a small (less than 2%) bump in the velocity at cell JC. For this reason, we set Q equal zero on each side of JC (Figures 30). The heat conduction terms used for each material in its corresponding energy equation were also set to zero on the sides of JC which resulted in little or no change in the mesh values.

At first, an attempt was made to change x_1 to its new value by using an interpolated velocity at x_1 to find its change in one time step. This gave large, though bounded, oscillations for all the mesh values at JC, and these oscillations moved along with the propagating shock and rarefaction. The reason for this very poor result can be seen as follows.

As the value of x_2 becomes small, the mass of material two, m_2, in cell JC also becomes small and unless calculated very accurately, the two values will combine to give a poor value of density, which then gives poor pressures, which in turn lead to poor velocity and energy values. To eliminate these difficulties, the following scheme was devised. As x_2 and m_2 approach zero, we wish the new value of x_2 to be such that $\frac{m_2}{x_2}$ will approach ρ_{JC+1}. Also, as x_1 and m_1 approach zero, we want $\frac{m_1}{x_1}$ to approach ρ_{JC-1}. When both x_1 and x_2 have values appreciably different from zero, we wish to combine the above two relations to obtain a mean value. Let $X_1 \equiv \frac{m_1}{\rho_{JC-1}}$ and $X_2 \equiv \frac{m_2}{\rho_{JC+1}}$; then the desired relation for x_1 at the next time step is given by

$$x_1^{n+1} = \frac{x_1^n(\delta x - X_2) + x_2^n(X_1)}{x_1^n + x_2^n}$$

or since $\delta x = x_1 + x_2$,

$$x_1^{n+1} = \frac{x_1^n(\delta x - m_2/\rho_{JC+1}) + (\delta x - x_1^n)(m_1/\rho_{JC-1})}{\delta x} \qquad (14)$$

All values on the right of Eq. (14) are obtained from the mesh at the end of the $n + 1$ calculation. Equation (14) insures that the densities in the interface cell will be compatible with the densities in the corresponding non-interface cells contiguous to JC. Figure 30 indicates that this method of calculating x_1^{n+1} gives the desired result for the return to Eqs. (4), (5), and (6) and the start of a new time cycle.

-59-

There are two methods which may be used to determine whether or not the interface cell should be changed after Eq. (14) has been calculated. For the material with the smallest volume, one would test to see if the mass or volume of this material is likely to go to zero in the next time cycle. For example, let $x_1^{n+1} < \frac{\delta x}{2}$. The change in volume in one time step is given by $\delta x_1 = x_1^{n+1} - x_1^n$. If $\delta x_1 \geq 0$, then x_1 is not decreasing with time and there should be no chance of JC changing. If $\delta x_1 < 0$, then x_1 is decreasing and there is a possibility of JC changing. Thus, for $\delta x_1 < 0$, if $(x_1^{n+1} + 1.03\ \delta x_1) \leq 0$, the cell should change and if > 0, the cell should not change. The factor 1.03 is used only as an example. The excess over one of this factor is included to account for accelerations. To test for a cell change by using $m_1 (x_1^{n+1} < \frac{\delta x}{2})$, the most appropriate method is to calculate by Eq. (4) for material one if all of mass one will flow out of JC when we go to start a new cycle. Similar statements apply when $x_1^{n+1} > \frac{\delta x}{2}$ for material two. The above test on mass was made in the diaphragm problem. The test on volume takes less machine time and is more appropriate for two dimensions. Equation (14) is the same for two dimensions where x_1 becomes the volume of material one, δx becomes the total volume of the interface cell, ρ_{JC+1} becomes the density of the nearest non-interface cell of type two material, and ρ_{JC-1} becomes the density of the nearest non-interface cell of type one material. When changing interface cells in one or two dimensions, one applies the conservation of mass, momentum, and energy to each material.

The calculation of x_1^{n+1} represents a volume and density change since there is no mass flow in this boundary calculation. Since $x_1 + x_2 = \delta x = a$ const., $\delta x_1 = -\delta x_2$. Let $\bar{p}$ be the pressure at the interface. The work done on material one is $-\bar{p}\delta x_1$ and the work done on material two is $+\bar{p}\delta x_1$. Let $\mathcal{E}_1$ and $\mathcal{E}_2$ be the internal energy per unit mass in JC for material one and material two, respectively. We thus replace $\mathcal{E}_1$ by $\mathcal{E}_1 - \dfrac{\bar{p}\delta x_1}{m_1}$ and $\mathcal{E}_2$ by $\mathcal{E}_2 + \dfrac{\bar{p}\delta x_1}{m_2}$ in the interface cell. In the diaphragm problem (Figure 30), $\bar{p}$ was calculated as the pressure in JC $\left(p_{JC} = \dfrac{{}_1p + {}_2p}{2} \right)$ using the values of $\mathcal{E}_1$ and $\mathcal{E}_2$ which were in the mesh after the completion of the $n + 1$ calculation. Since the flow is to the right in the diaphragm, the values of $\mathcal{E}_1$ and $\mathcal{E}_2$ are high and low, respectively, at the end of the $n + 1$ calculation. The resultant inaccuracy in $\bar{p}$ gives the small variations of the calculated density and temperature near the interface (Figure 30). Though it has not been tried, it appears that the calculation of $\bar{p}$ as $\bar{p} = \dfrac{p_{JC+1} + p_{JC-1}}{2}$ would resolve this difficulty in the internal boundary calculation. Of course, the value of p_{JC} obtained in the $n + 1$ calculation could be saved and used for the value of $\bar{p}$. This was done in a similar calculation and found to give good results. If $\bar{p}$ is a given function of space and time on an external boundary, then the above method will allow the correct amount of work to be done on the system.

A difficulty in the diaphragm problem (Figure 30) may be noted. The shock front is about six cells wide as compared to approximately

three cells for the infinite shock in the piston problem. This indi-
cates the selected difference scheme will have difficulty following
weak shocks.

A cycle consists of the n + 1 calculation and the boundary
calculation. The boundary calculation consists of a volume change,
the possibility of a cell change, and the internal energy changes.

CHAPTER II

DIFFERENCING IN TWO DIMENSIONS

Equations (1), (2), and (3) in cylindrical coordinates with no angular dependence may be written as

$$\frac{\partial \rho}{\partial t} = - \frac{\partial (r\rho u)}{r \partial r} - \frac{\partial (\rho v)}{\partial z} \tag{15}$$

$$\frac{\partial (\rho u)}{\partial t} = - \frac{\partial p}{\partial r} - \frac{\partial (r\rho uu)}{r \partial r} - \frac{\partial (\rho vu)}{\partial z} \tag{16}$$

$$\frac{\partial (\rho v)}{\partial t} = - \frac{\partial p}{\partial z} - \frac{\partial (r\rho uv)}{r \partial r} - \frac{\partial (\rho vv)}{\partial z} \tag{17}$$

$$\frac{\partial (\rho E)}{\partial t} = - \frac{\partial (r\rho u)}{r \partial r} - \frac{\partial (pv)}{\partial z} - \frac{\partial (r\rho uE)}{r \partial r} - \frac{\partial (\rho vE)}{\partial z} \tag{18}$$

where u and v are the r- and z-components of the velocity.

We will difference these equations for the mesh represented in Figure 32. The radius at the center of each cell is given by r_i = $\delta r(i - 1/2)$ and at the sides by $r_{i+1/2} = i\delta r$ and $r_{i-1/2} = (i - 1)\delta r$. In this notation, the volume and areas of the cell (i,j) are given by

$$V_i^j = 2\pi r_i \delta r \delta z$$

$$A_i^{j-1/2} = A_i^{j+1/2} = 2\pi r_i \delta r$$

$$A_{i-1/2} = 2\pi r_{i-1/2} \delta z$$

$$A_{i+1/2} = 2\pi r_{i+1/2} \delta z$$

$$(19)$$
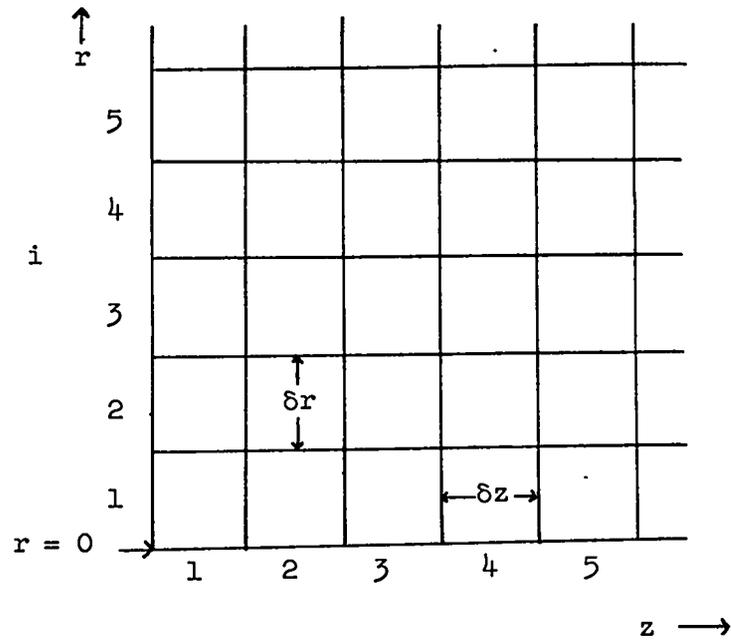
Figure 32

from which

$$\left.\begin{array}{l} \dfrac{A_i^{j-1/2}}{V_i^j} = \dfrac{A_i^{j+1/2}}{V_i^j} = \dfrac{1}{\delta z} \\[4mm] \dfrac{A_{i-1/2}^j}{V_i^j} = \dfrac{r_{i-1/2}}{r_i \delta r} \\[4mm] \dfrac{A_{i+1/2}^j}{V_i^j} = \dfrac{r_{i+1/2}}{r_i \delta r} \end{array}\right\} \qquad (20)$$

Differencing Eq. (15) we get

$$\rho_i^{j\,n+1} - \rho_i^{j\,n} = \delta t \left[\frac{r_{i-1/2}\,\rho_{i-1/2}^j\,u_{i-1/2}^j - r_{i+1/2}\,\rho_{i+1/2}^j\,u_{i+1/2}^j}{r_i \delta r} \right.$$

$$\left. + \frac{\rho_i^{j-1/2}\,v_i^{j-1/2} - \rho_i^{j+1/2}\,v^{j+1/2}}{\delta z} \right] \qquad (21)$$

where all mesh values on the right are at time step n. By Eq. (20),
Eq. (21) may be written as

$$\rho_i^{j\,n+1} - \rho_i^{j\,n} = \frac{\delta t}{V_i^j} \left[A_{i-1/2}^j\,\rho_{i-1/2}^j\,u_{i-1/2}^i - A_{i+1/2}^j\,\rho_{i+1/2}^j\,u_{i+1/2}^j \right.$$

$$\left. + A_i^{j-1/2}\,\rho_i^{j-1/2}\,v_i^{j-1/2} - A_i^{j+1/2}\,\rho_i^{j+1/2}\,v_i^{j+1/2} \right]$$

or simply

$$\rho_i^{j^{n+1}} - \rho_i^{j^n} = \frac{\delta t}{V_i^j} \left[(A\rho u)_{i-1/2}^j - (A\rho u)_{i+1/2}^j + (A\rho v)_i^{j-1/2} - (A\rho v)_i^{j+1/2} \right] \quad (22)$$

Another method to obtain Eq. (22) is to integrate Eq. (1) over the volume, V_i^j, convert the right side by Gauss' theorem to a surface integral, and approximate the result assuming V_i^j is small. This latter method of evaluation of the divergence is also easy when other coordinate systems are to be used. To simplify the notation, we will designate quantities at i, j - 1/2 as side one, at i - 1/2, j as side two, at i, j + 1/2 as side three, and at i + 1/2, j as side four. Thus, Eq. (22) is written as

$$\rho_i^{j^{n+1}} - \rho_i^{j^n} = \frac{\delta t}{V_i^j} \left[(A\rho u)_2 - (A\rho u)_4 + (A\rho v)_1 - (A\rho v)_3 \right] \quad (23)$$

or if mass is carried in each cell instead of density

$$M_i^{j^{n+1}} - M_i^{j^n} = \delta t \left[(A\rho u)_2 - (A\rho u)_4 + (A\rho v)_1 - (A\rho v)_3 \right] \quad (24)$$

where $M_i^j = \rho_i^j V_i^j$. The $(A\rho u)$ or $(A\rho v)$ terms are called the mass flow terms. They are the mass per unit time flowing across their respective sides of the cell. If one starts at i = 1 and j = 1 with suitable boundary conditions, then we need to calculate values for the flow quantities only on sides three and four. Other similarities to the one-dimensional cases are used, i.e., values on sides one and three are differenced as

in one dimension in the j direction for each i, and values on sides two and four are differenced in the i direction for each j. In Eq. (24), mass is seen to be conserved as in the one-dimensional case. Equations (16), (17), and (18) are differenced similar to Eq. (15) and give

$$\rho_i^{j^{n+1}} u_i^{j^{n+1}} - \rho_i^{j^n} u_i^{j^n} = \frac{\delta t}{V_i^j} \left[\frac{V_i^j}{\delta r} (p_2 - p_4) + (A\rho u)_2 \, u_2 \right.$$

$$\left. - (A\rho u)_4 \, u_4 + (A\rho v)_1 \, u_1 - (A\rho v)_3 \, u_3 \right] \qquad (25)$$

$$\rho_i^{j^{n+1}} v_i^{j^{n+1}} - \rho_i^{j^n} v_i^{j^n} = \frac{\delta t}{V_i^j} \left[\frac{V_i^j}{\delta z} (p_1 - p_3) + (A\rho u)_2 \, v_2 - (A\rho u)_4 \, v_4 \right.$$

$$\left. + (A\rho v)_1 \, v_1 - (A\rho v)_3 \, v_3 \right] \qquad (26)$$

and

$$\rho_i^{j^{n+1}} E_i^{j^{n+1}} - \rho_i^{j^n} E_i^{j^n} = \frac{\delta t}{V_i^j} \left[(A p u)_2 - (A p u)_4 + (A p v)_1 - (A p v)_3 \right.$$

$$\left. + (A\rho u)_2 \, E_2 - (A\rho u)_4 \, E_4 + (A\rho v)_1 \, E_1 - (A\rho v)_3 \, E_3 \right] \qquad (27)$$

In the two-dimensional example to be presented below, the differencing is like the scheme selected for the diaphragm problem. The ρ's, v's, and u's for mass flow terms were calculated by Type III differencing. p_4 is the sum of the material pressure on side four and the "cut off"

value of Q computed with the u's on side four. Similarly, p_3 is a sum on side three using the v's in the velocity gradient portion of the viscosity calculation. The pressure times velocity terms in Eq. (27) are computed as the sum of the heat conduction term and of the above pressures times the velocities used in mass flow. This sum is then multiplied by the proper area so that the equivalent differential term which has been added to Eq. (3) is $\nabla \cdot C_2 \underset{E}{D} \nabla \ell$. The u's, v's, and E's which multiply the mass flow terms are differenced as Type II with the corresponding mass flow term as the flow test number, V_T. Q is zero at r = 0.

The two-dimensional steady state test problem geometry is shown in Figure 33. We wish to determine the axially symmetric flow about a flat-nosed cylinder within a cylindrical pipe. The flow of the polytropic gas enters on the left side with a Mach number (M) of 1.58, density and sound speed equal 1.0, and $\gamma = 1.4$. All cells to the right of j = 14 were assumed to have the same mesh values as those with the corresponding value of i in cell j = 14. The pipe and obstruction had rigid walls. Unfortunately, the code was written for the fixed configuration of Figure 33 and for $\delta z = \delta r = 1.0$. The left boundary was not far enough upstream to prevent perturbations near the input (see Figures 33, 34, 35, 36, and 37) close to the axis. Figures 34, 35, 36, 37, and 38 show the input conditions which were held fixed in the j = 0 cells. The flat line in j = 0 was drawn to indicate that the input values of ρ, u, v, and Θ were used for the corresponding value on the right boundary of this cell.

Considering these perturbations and the coarseness of the mesh, it seems remarkable that certain average results were obtained. The position[5] of the detached shock is represented by the solid line in Figure 33. The limits[6] of the force on the flat-nosed cylindrical face are 387.0 and 336.4. This gives a most probable experimental value of 361.70. The calculated value at steady state (Figure 40) for this problem gave a corresponding value of 354.0, i.e., about 2% low. In Figures 33 to 39, the mesh values at a time of about 40 are plotted. The steady state seemed to be reached at a time of about 20 (see Figure 40), which required about 45 minutes calculation time. The calculation to the time of about 40 was performed to see if these perturbations of the mesh values near the input would cause any change in the steady state values. No change was observed. As an admittedly rough criterion for locating the shock position, we may take the position of one-half height on the density curves (Figure 34). They are plotted in Figure 33. The perturbation near the input is evident. The coarseness of the mesh and the presence of diffusion terms seem to cause the shock and reflected shock at the outside wall to lose their respective identities and to produce an average position. In an effort to find some quantity which might serve to differentiate between the shock and reflected shock, we have plotted in Figure 39 the tangent angle of the velocity vector. Since no sudden change in slope is observed, it is evident that this quantity does not serve the purpose. Unfortunately, no other single quantity examined has proved useful in this connection. It should be noted, however, that despite the crudity
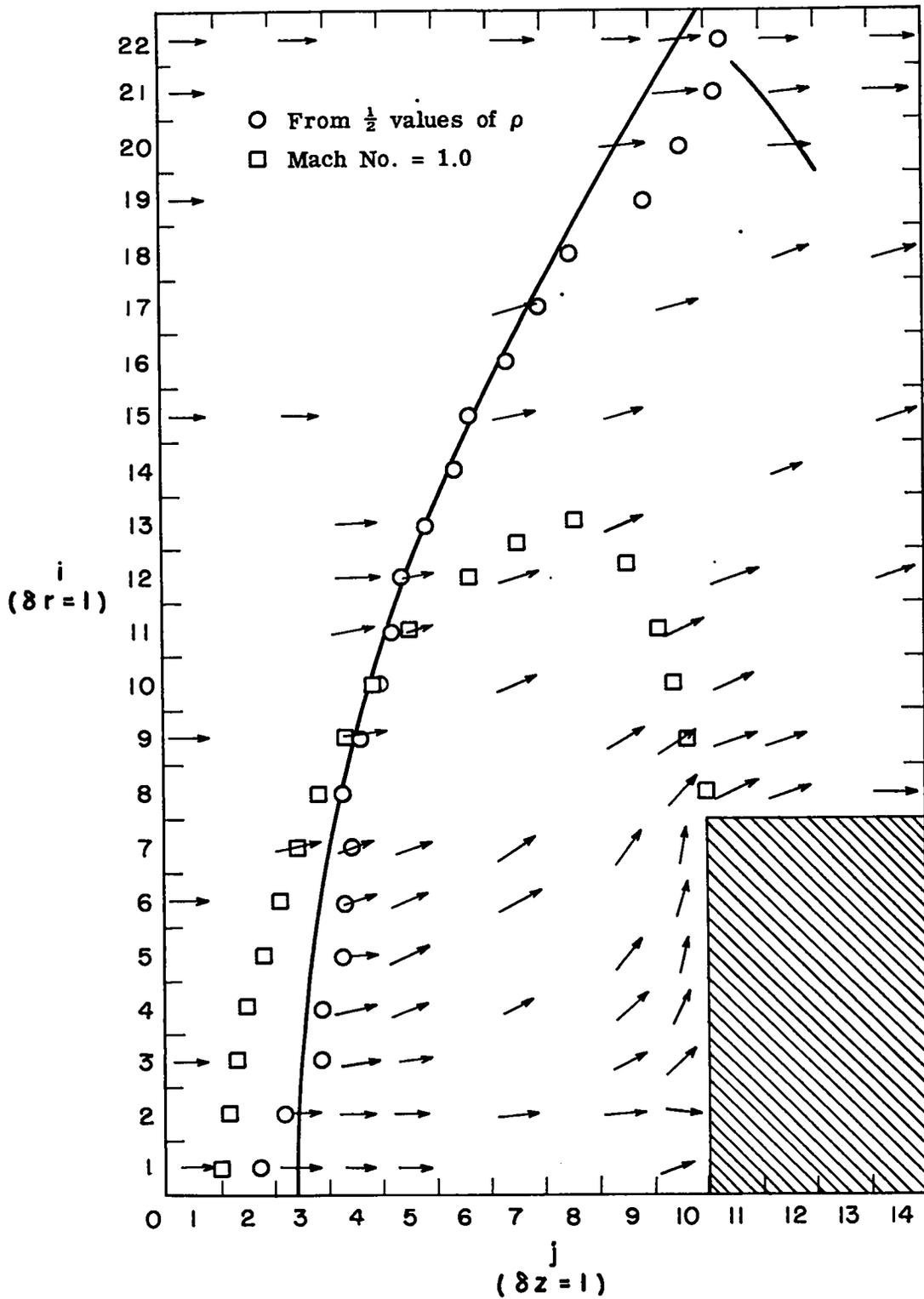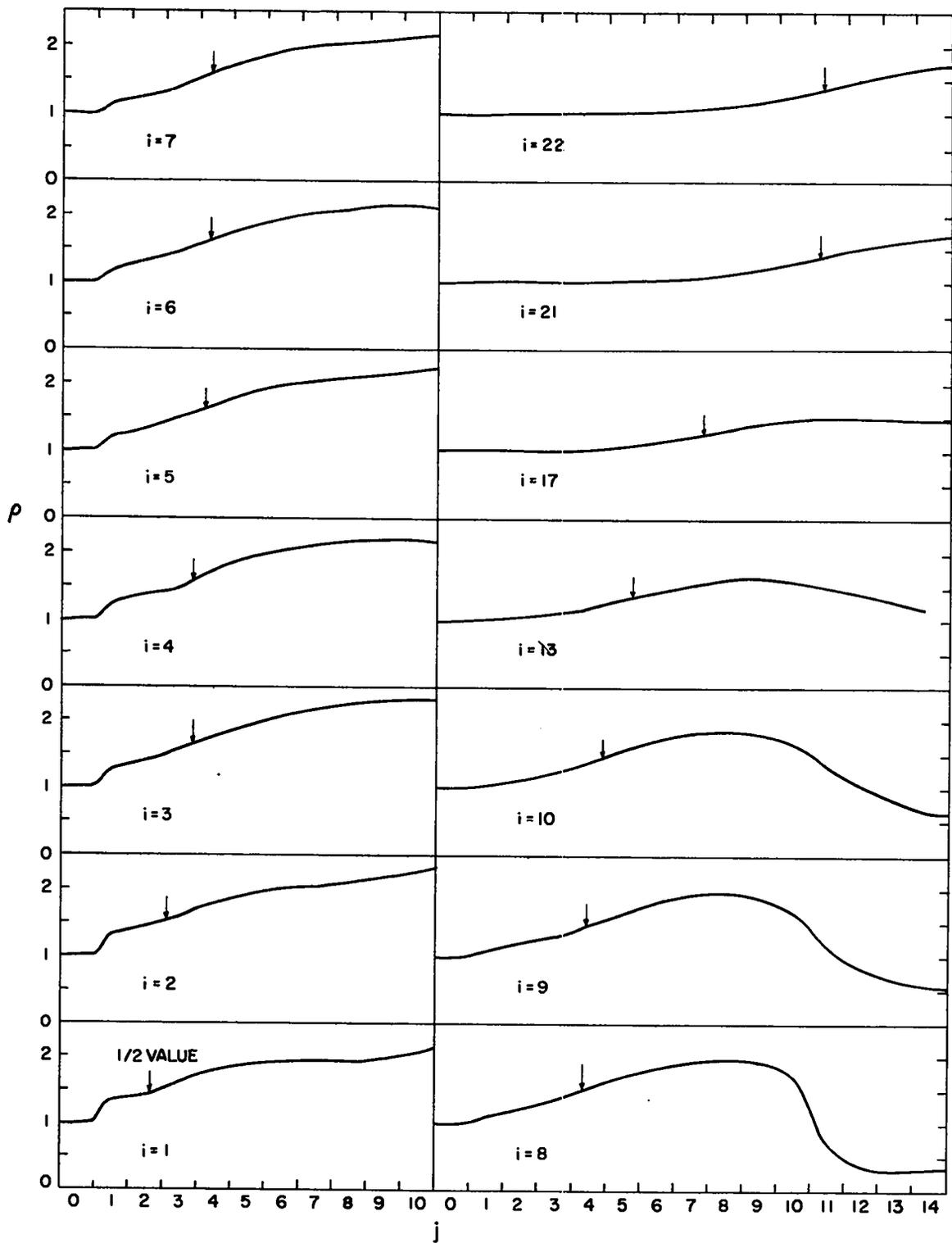
Figure 33
-70-
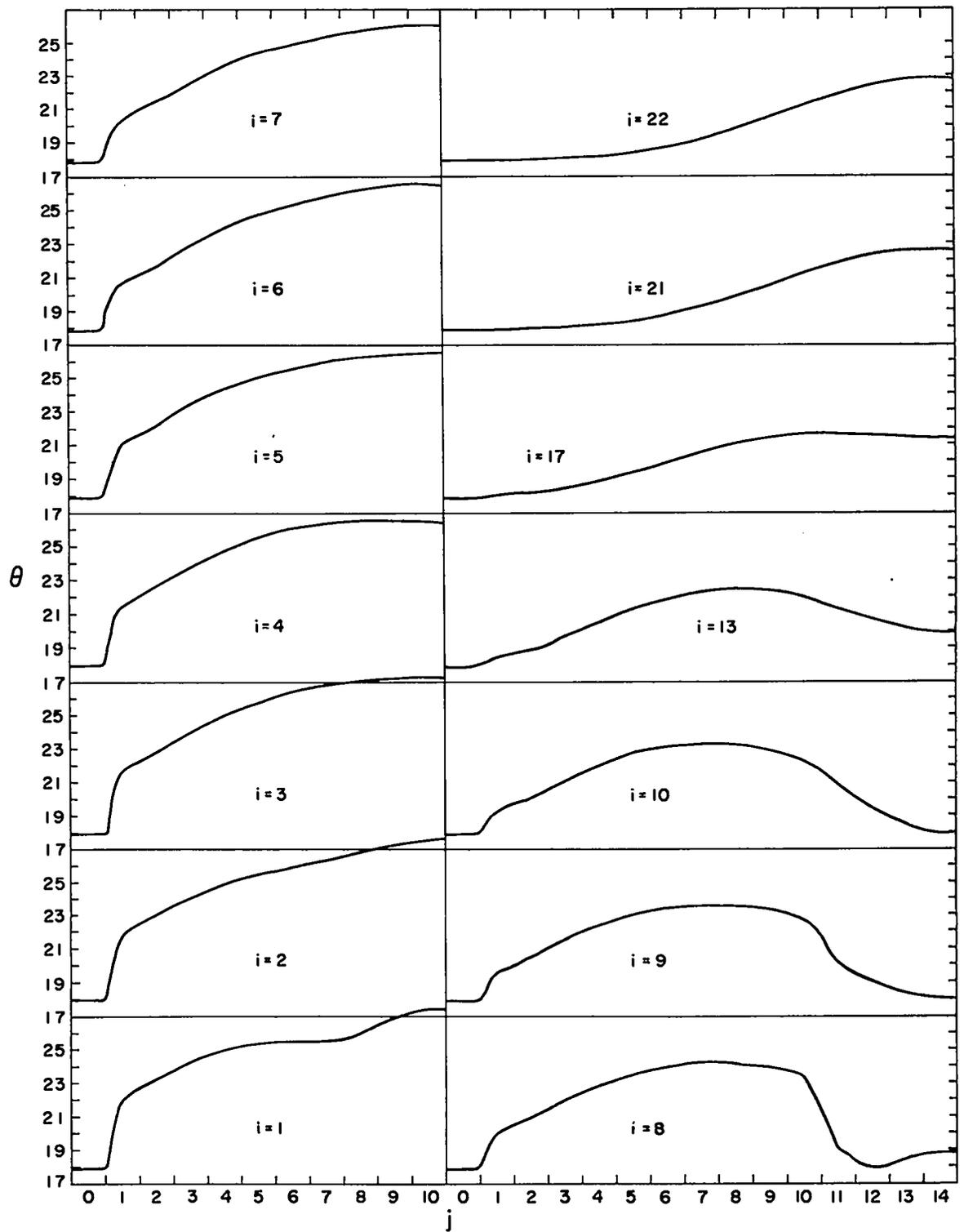
Figure 34
-71-

Figure 35
-72-
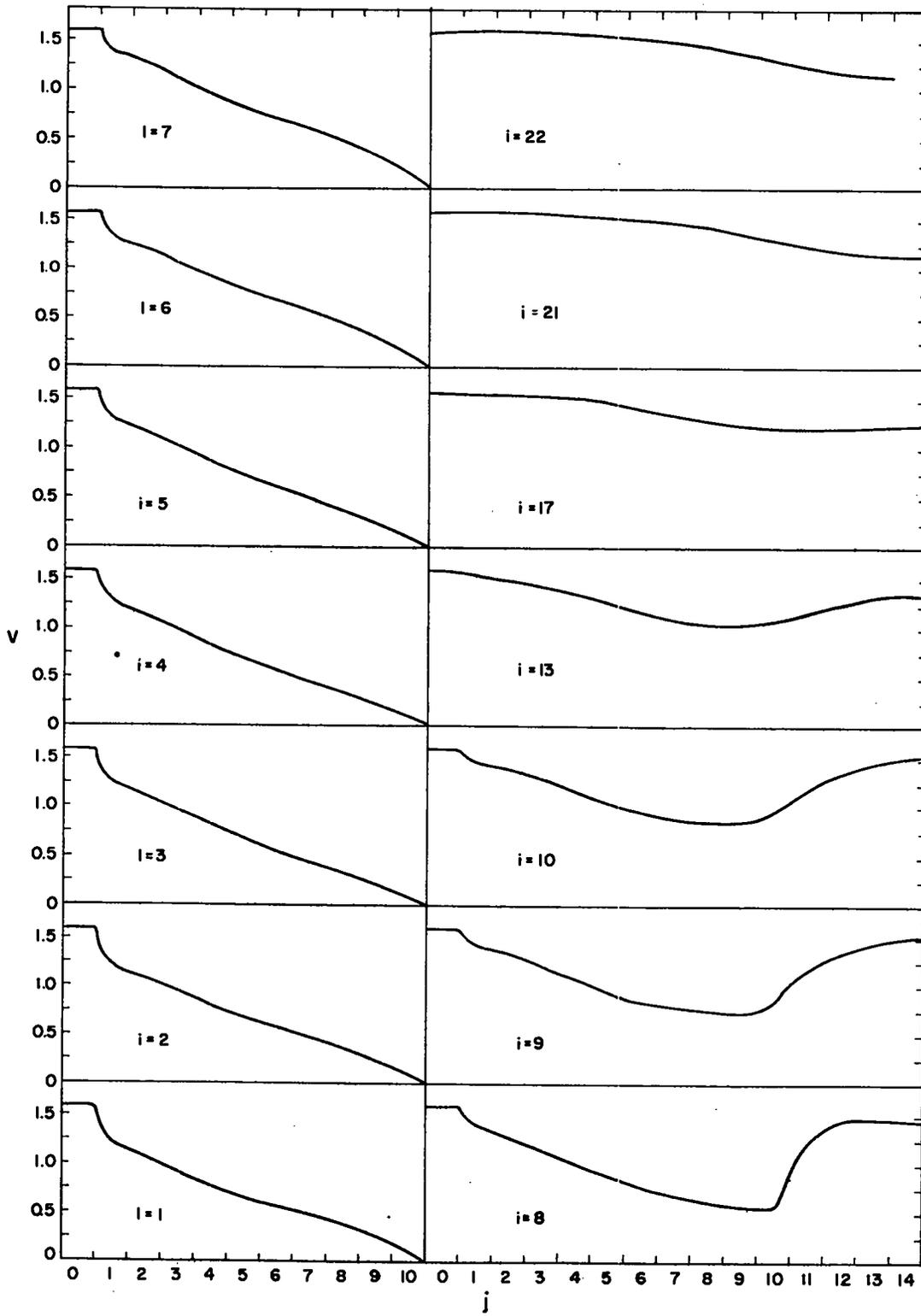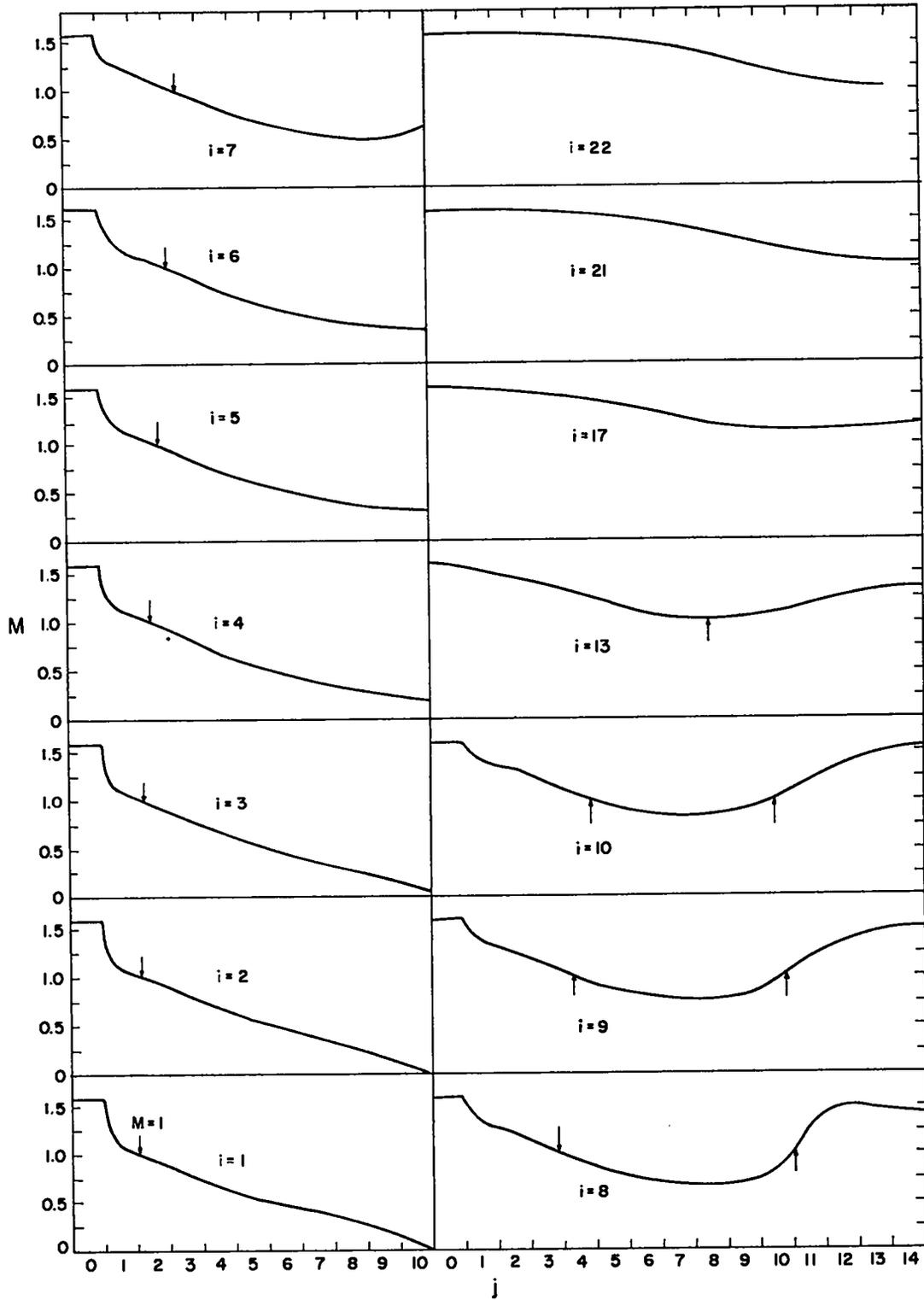
Figure 36
-73-

Figure 37
-74-
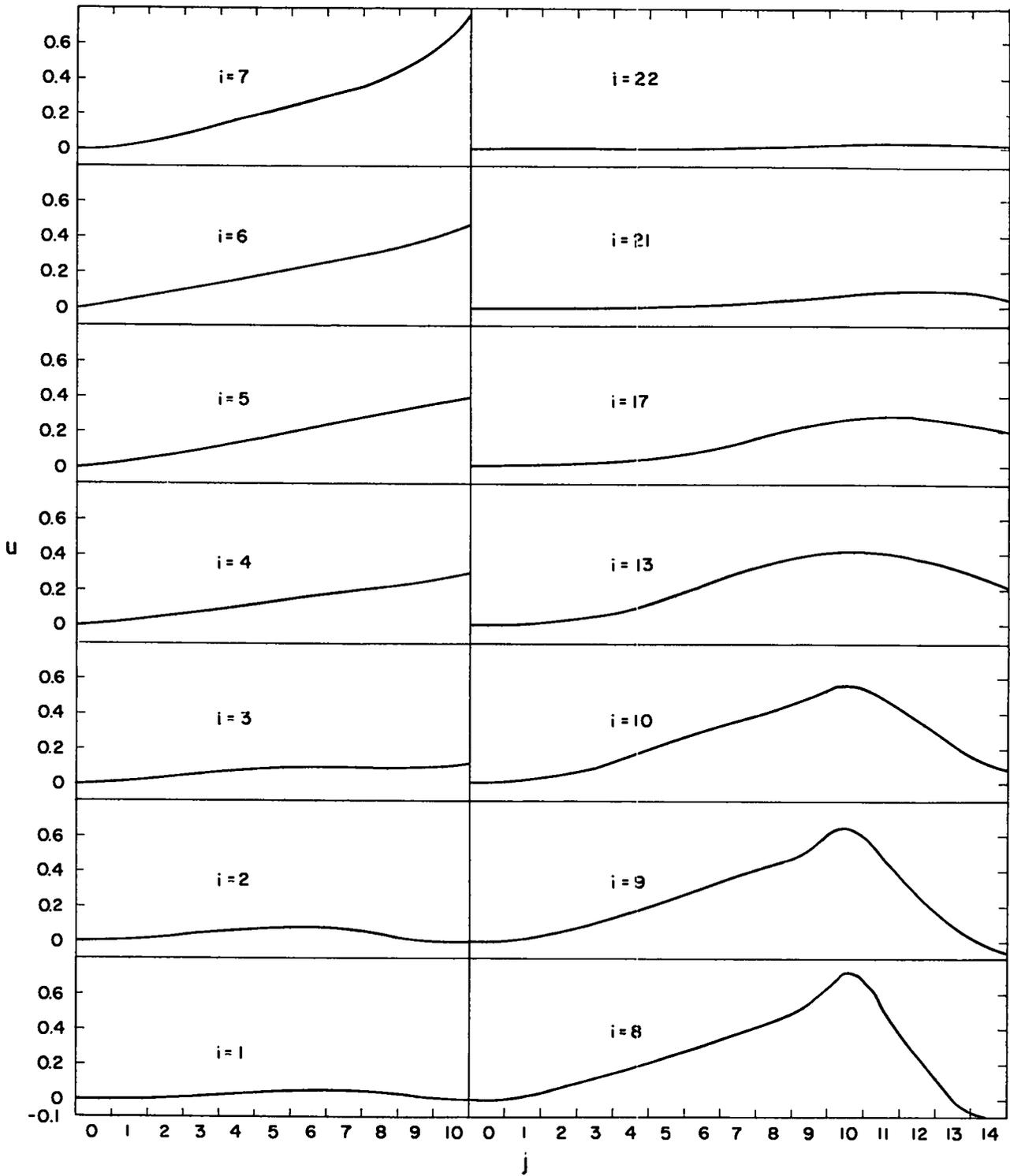
Figure 38
-75-
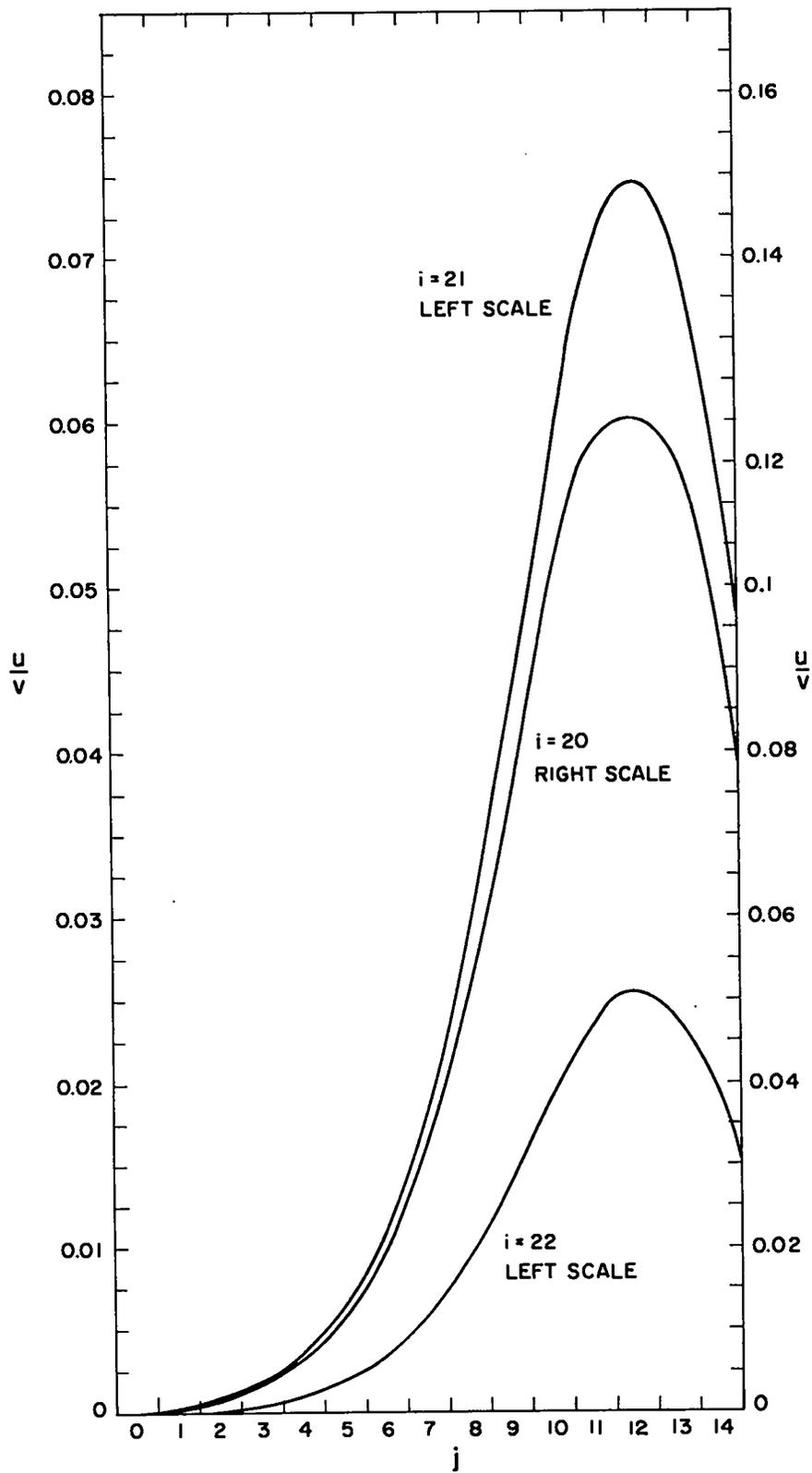
Figure 39
-76-
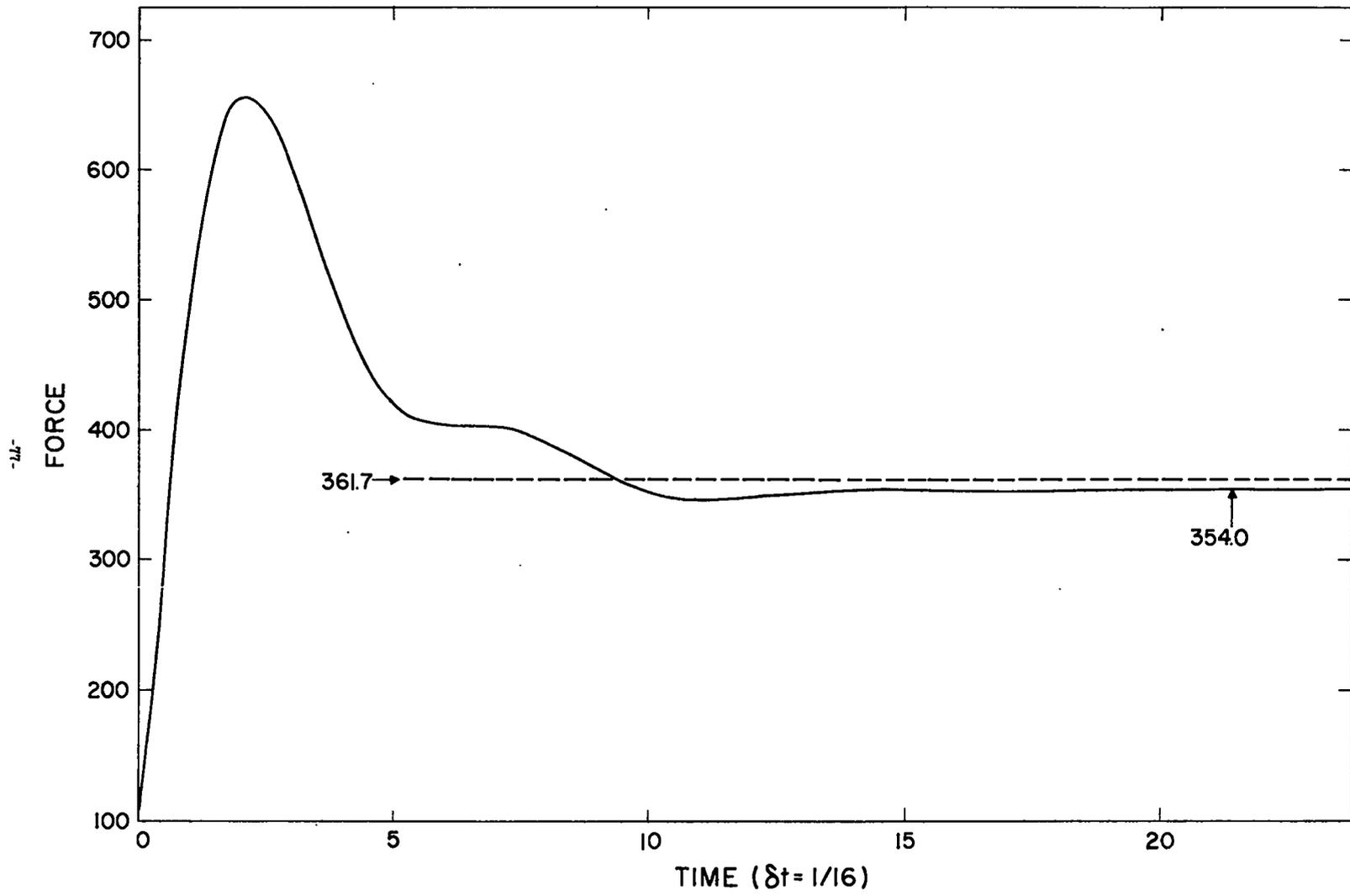
Figure 40

of the one-half height criterion, the position of the shock front is correct to within a cell size. The calculated sonic line in Figure 33 was obtained from plots of the Mach number (Figure 37). The vectors in Figure 33 show the direction of flow but not the magnitude (see Figures 36 and 38). The normal component of the velocity in the cells next to the flat-nosed surface extrapolates to zero (Figure 36). The spread of about six cells in this weak shock is again evident as it was in the diaphragm problem.

For a two-dimensional problem which has a moving interface between materials (Figure 41), the only new difficulty introduced is that of calculating the partial areas for the mass flow and work (pV) terms. The criterion that each interface cell must have two, and only two, adjoining interface cells leads to six types of three interface cell combinations (Figure 41). To maintain the interface normal to outside boundary walls will require special interface cell types. These special cells should be maintained such that only one interface cell will be next to an outside boundary where the interface terminates. Two interface cells at i = 1 (with consecutive j values), for example, would violate the above criterion. The conservation of mass for each material will be given by (see Eq. (24))

$$
M_{i}^{1,n+1} - M_{i}^{1,n} = \delta t \left[(A\rho u)_{2}^{1} - (A\rho u)_{4}^{1} + (A\rho v)_{1}^{1} - (A\rho v)_{3}^{1} \right] \quad (28)
$$

and
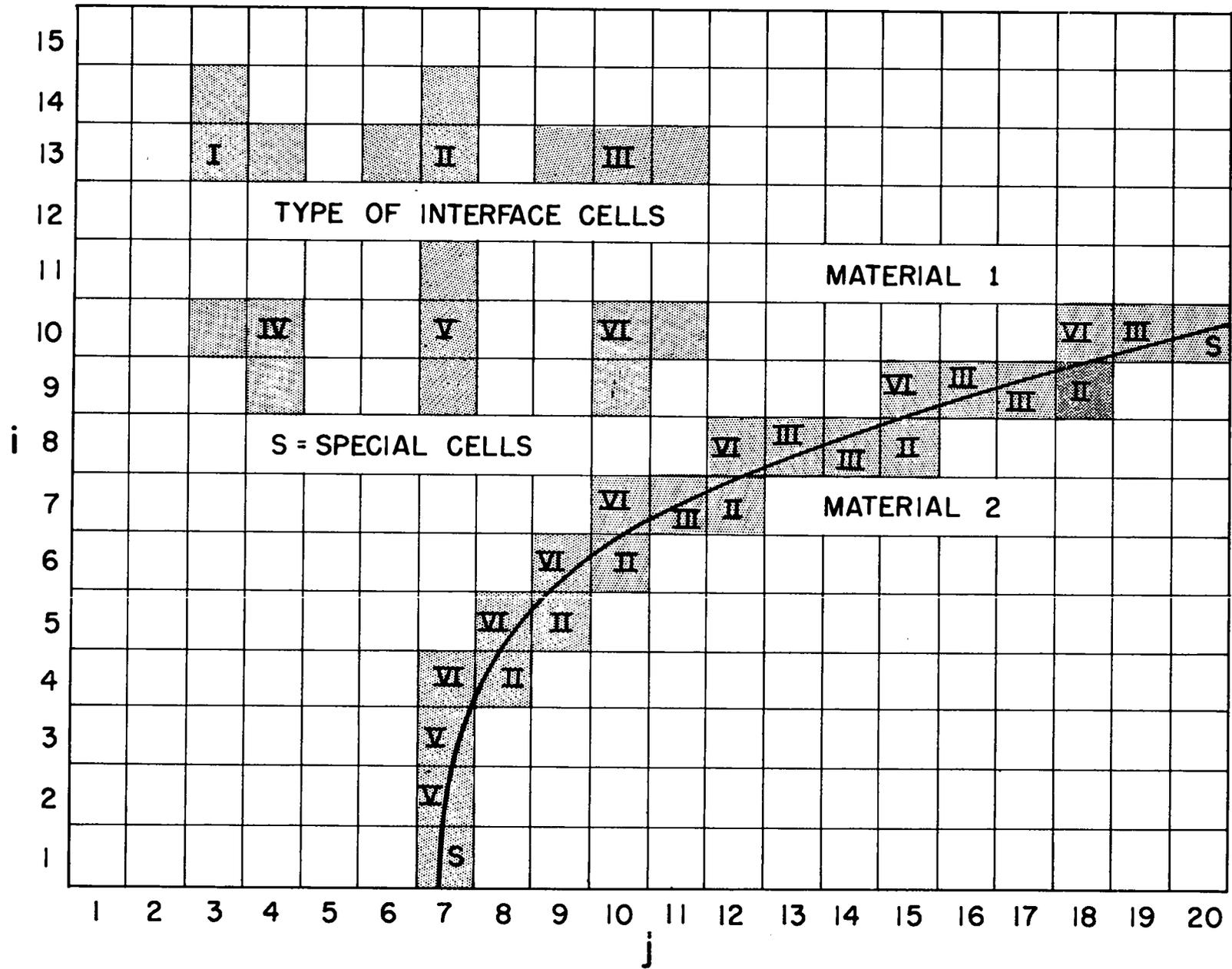
Figure 41

$$M_i^{2,j,n+1} - M_i^{2,j,n} = \delta t \left[(A\rho u)_2^2 - (A\rho u)_4^2 + (A\rho v)_1^2 - (A\rho v)_3^2 \right] \tag{29}$$

where the superscripts 1 or 2 indicate the material. As an illustration of the evaluation of the mass flow terms in Eqs. (28) and (29), consider a Type I interface cell in (i,j) with material 1 to the right and above and with material 2 to the left and below. In this case, $A_1^1 = 0$, $A_2^1 = 0$, $A_1^2 = A_1$, and $A_2^2 = A_2$. A scheme must now be devised to calculate one of the partial areas on side three and side four since $A_3 = A_3^1 + A_3^2$ and $A_4 = A_4^1 + A_4^2$. The simplest scheme appears to be given by using a linear combination of the partial volumes, i.e.,

$$A_3^2 = \frac{V_i^{2,j} + V_i^{2,j+1}}{2\delta z}$$

and

$$A_4^1 = \frac{V_i^{1,j} + V_{i+1}^{1,j}}{2\delta r}$$

Other schemes which use the given partial volumes in several cells and attempt curve fits lead to quadratic, cubic, and higher order equations which should be avoided if possible. A code is being prepared which uses the simple scheme mentioned above. This code will calculate the values of the density on the cell boundary which joins two interface cells by Type I differencing and will use Type III differencing with extrapolation elsewhere. The values of u and v are continuous through the interface

and are to be calculated as before. Pressures are calculated as in the diaphragm problem. The viscosity and heat conduction terms are to be zero at the boundary of any interface cell. Equations (25) and (26) for an interface cell become.

$$
\begin{aligned}
\left(\overset{1,n+1}{M_i^j} + \overset{2,n+1}{M_i^j} \right) u_i^{j,n+1} - \left(\overset{1,n}{M_i^j} + \overset{2,n}{M_i^j} \right) u_i^{j,n} &= \delta t \left[\frac{v_i^j}{\delta r} (p_2 - p_4) \right. \\
&+ \left\{ \overset{1}{(A\rho u)_2} + \overset{2}{(A\rho u)_2} \right\} u_2 - \left\{ \overset{1}{(A\rho u)_4} + \overset{2}{(A\rho u)_4} \right\} u_4 \\
&+ \left. \left\{ \overset{1}{(A\rho v)_1} + \overset{2}{(A\rho v)_1} \right\} u_1 - \left\{ \overset{1}{(A\rho v)_3} + \overset{2}{(A\rho v)_3} \right\} u_3 \right]
\end{aligned} \tag{30}
$$

and

$$
\begin{aligned}
\left(\overset{1,n+1}{M_i^j} + \overset{2,n+1}{M_i^j} \right) v_i^{j,n+1} - \left(\overset{1,n}{M_i^j} + \overset{2,n}{M_i^j} \right) v_i^{j,n} &= \delta t \left[\frac{v_i^j}{\delta z} (p_1 - p_3) \right. \\
&+ \left\{ \overset{1}{(A\rho u)_2} + \overset{2}{(A\rho u)_2} \right\} v_2 - \left\{ \overset{1}{(A\rho u)_4} + \overset{2}{(A\rho u)_4} \right\} v_4 \\
&+ \left. \left\{ \overset{1}{(A\rho v)_1} + \overset{2}{(A\rho v)_1} \right\} v_1 - \left\{ \overset{1}{(A\rho v)_3} + \overset{2}{(A\rho v)_3} \right\} v_3 \right]
\end{aligned} \tag{31}
$$

Equation (27) must be solved for each material; thus, it takes the following form:

$$
\overset{1,n+1}{M_i^j} \overset{1,n+1}{E_i^j} - \overset{1,n}{M_i^j} \overset{1,n}{E_i^j} = \delta t \left[\overset{1}{(A\rho u)_2} \overset{1}{E_2} - \overset{1}{(A\rho u)_4} \overset{1}{E_4} + \overset{1}{(A\rho v)_1} \overset{1}{E_1} - \overset{1}{(A\rho v)_3} \overset{1}{E_3} \right.
$$
$$
\left. + \left\{ \overset{1}{(A\rho u)_2} - \overset{1}{(A\rho u)_4} + \overset{1}{(A\rho v)_1} - \overset{1}{(A\rho v)_3} \right\} \right] \tag{32}
$$

$$\overset{2}{M}{}_i^{j\,,n+1}\,\overset{2}{E}{}_i^{j\,,n+1} - \overset{2}{M}{}_i^{j\,,n}\,\overset{2}{E}{}_i^{j\,,n} = \delta t \left[\overset{2}{(A\rho u)}{}_2\,\overset{2}{E}{}_2 - \overset{2}{(A\rho u)}{}_4\,\overset{2}{E}{}_4 + \overset{2}{(A\rho v)}{}_1\,\overset{2}{E}{}_1 - \overset{2}{(A\rho v)}{}_3\,\overset{2}{E}{}_3 \right.$$

$$\left. + \left\{ \overset{2}{(A\rho u)}{}_2 - \overset{2}{(A\rho u)}{}_4 + \overset{2}{(A\rho v)}{}_1 - \overset{2}{(A\rho v)}{}_3 \right\} \right] \tag{33}$$

The cycling of this problem would be as follows: One first calculates the values at time $n + 1$ for the whole mesh using Eqs. (23), (25), (26), and (27) for non-interface cells and Eqs. (28), (29), (30), (31), and (33) for interface cells. Then the calculations are made for each interface cell of the moving boundary. These calculations give the new values of the partial volumes, the interface cell changes, and the new values of the internal energy resulting from the volume change. The cycle is then repeated. This procedure is merely the two-dimensional analogue of the method used in the diaphragm problem.

REFERENCES

1. J. von Neumann and R. D. Richtymyer, J. Appl. Phys. 21, 232 (1950).

2. Rolf Landshoff, Los Alamos Report LA-1930 (1955).

3. Martha W. Evans and Francis H. Harlow, Los Alamos Report LA-2139 (1957).

4. Francis H. Harlow, Los Alamos Report LAMS-1956 (1955).

5. B. W. Marschner, A. E. Thesis, California Institute of Technology (1948).

6. S. F. Hoerner, Aerodynamic Drag, p. 222 (1951).